Title
The Impact of Homologous Recombination on Silent Chromatin in Saccharomyces cerevisiae

Author
Sieverman, Kathryn Jeanne

Publication Date
2017

Peer reviewed|Thesis/dissertation

The Impact of Homologous Recombination on Silent Chromatin in *Saccharomyces cerevisiae*

by

Kathryn Jeanne Sieverman

A dissertation submitted in partial satisfaction of the

requirements for the degree of

Doctor of Philosophy

in

Molecular and Cell Biology

in the

Graduate Division

of the

University of California, Berkeley

Committee in charge:

Professor Jasper Rine, Chair
Professor Elçin Ünal
Professor Douglas Koshland
Professor Kathleen Ryan

Fall 2017

The Impact of Homologous Recombination on Silent Chromatin in *Saccharomyces cerevisiae*

by Kathryn Jeanne Sieverman

Abstract

The Impact of Homologous Recombination on Silent Chromatin in *Saccharomyces cerevisiae*

by

Kathryn Jeanne Sieverman

Doctor of Philosophy in Molecular and Cell Biology

University of California, Berkeley

Professor Jasper Rine, Chair

Specialized chromatin domains repress transcription of genes within them and present a barrier to many DNA-protein interactions. Silent chromatin in the budding yeast *Saccharomyces cerevisiae*, akin to heterochromatin of metazoans and plants, is imparted by the Silent Information Regulation (SIR) proteins, Sir1-Sir4. Silencing is well described at the *HML* and *HMR* loci in *S. cerevisiae*, which harbor un-expressed copies of the genes necessary for mating-type identity. SIR-silenced chromatin inhibits transcription of PolII- and PolIII-transcribed genes, yet somehow grants access to proteins necessary for DNA transactions such as replication and homologous recombination. Homologous recombination within silent chromatin is a key aspect of yeast biology, as the process of mating-type switching depends upon it. Mating-type switching initiates with a programmed double-strand break at the *MAT* locus, which then accesses either *HML* or *HMR* to template homologous recombination and repair the double-strand break. Whether homologous recombination impacts the stability of silent chromatin at *HML* or *HMR* was not known when I began this study.

To investigate the impact of homologous recombination on silent chromatin, I developed an assay to detect even transient changes in the dynamics of transcriptional silencing at *HML* after it served as a template for homologous recombination. Homologous recombination specifically targeted to *HML* often led to transient loss of transcriptional silencing at *HML*. Interestingly, many cells could template homology-directed repair at *HML* without an obligate loss of silencing, even in recombination events with extensive gene conversion tracts. Thus, recombination with *HML* led to two distinct outcomes, one in which silent chromatin was disrupted enough to permit transcription, and one in which silencing persisted despite the presence of the homologous recombination machinery.

In the cells that experienced silencing loss following recombination, transcription persisted for two to three hours after all double-strand breaks were repaired. mRNA levels from cells that experienced recombination-induced silencing

loss did not approach the amount of mRNA seen in cells lacking transcriptional silencing. Thus, silencing loss at *HML* after homologous recombination was short-lived and limited.

I explored the possibility that chromatin-remodeling complexes known to play a role in homology-directed repair might affect the stability of silent chromatin after homologous recombination. Analysis in a background mutant for the SWI/SNF or INO80 chromatin-remodeling complexes revealed no clear role for nucleosome remodeling by these complexes in influencing the likelihood of silencing loss at *HML* associated with homologous recombination.

In the process of investigating post-recombination silencing loss, I found that the founder cell of a colony experienced a different likelihood of both silencing loss and gene conversion from its progeny. This manifested as colonies grown from single cells bearing cells that both maintained and lost silencing, as well as cells that both did and did not show evidence of homologous recombination. Thus, differences in both phenotype and genotype existed between a founder cell and its early progeny after double-strand break induction and repair.

The work in this dissertation has laid the foundational observations for further dissecting the processes that can disrupt what is otherwise a remarkably stable repressive chromatin structure.

Table of Contents

List of Figures

List of Tables

Acknowledgments

The journey underlying this body of work has transformed me into a wiser, more confident, and more productive scientist. I owe endless thanks to the people who have helped me along the way.

To Jasper, my advisor: I am beyond grateful for the wisdom and patience that you have continuously offered in your mentorship. I will always admire the care and compassion you give to each of your mentees, and I thank you for guiding me through graduate school. You have greatly shaped the way I think and write about science. Despite spending over five years under your wing, I feel there is much more that could be learned from you.

To my family, who have supported me wholeheartedly since day one: I love you dearly. I would not be here today without the unconditional love from my grandmother, Mammaw, who over the course of my graduate studies was diagnosed with and passed away from cancer. To my grandfather, Pawpaw – thank you for telling me how proud of me you are each time we talk on the phone. To my parents, Julie and Casey – thank you for your unwavering support. I am so grateful to have parents that I know I can count on for anything. To my sister, Claire – thank you for being one of my dearest friends and for all of the times you've made me smile. To Uncle Andy – thank you for your emails and texts that made Austin seem not too far away, and I promise one day soon I will make enough money to repay you for all of the lunches you've bought me. To my cousins Chris and Steve – thank you for all the meals and Grateful Dead concerts that made the Bay Area so quickly feel like home.

To Ryan Janke: the experiments in this study would not have made it this far without your selfless guidance and motivation. Words cannot express the gratitude I have for all of the time I've gotten to spend alongside you in the lab, and I will greatly miss having you as a colleague. Thank you for your after-hours pep talks and for always being a source of positivity in the lab. Your future mentees will be extremely fortunate to be working under for such a wonderful P.I.

To Anne Dodson: thank you for taking me under your introverted wing. From my first days as a rotation student to going on your first backpacking trip with you to watching you complete graduate school with such poise and productivity, I will never cease to be grateful for having someone so wonderful to always look up to.

To the Rine lab: I wouldn't change a thing about any of you. I am so lucky to have had such freaking stellar colleagues to work with. I will dearly miss our backpacking trips, funches, folly-making, and constant exchange of questionable jokes. I have learned so much from all of you, and am so grateful that many of my co-workers have also been my closest friends. Debbie, Dave, Sarah, Lauren, Anne, Aisha, David, Ryan, Gavin, Jean,

Kripa, Davis W., Willy Nilly, Daniel, Marc, Victoria, and Ellie – thank you for making the Rine lab the best lab to work on the whole planet.

To my thesis committee, Elçin, Doug, and Kathleen – thank you for your invaluable guidance and support. To Martin Kupiec – thank you for the brilliance and passion you brought to my project.

To my scientific mentors who got me here in the first place: Dave and Leslie, I will always cherish the time I spent in your lab. Thank you for granting me the opportunity to enter the world of biology research. I feel truly lucky for your guidance and camaraderie, and I hope to continue our hours-long conversations about life for years to come.

To my high school chemistry teachers, Casey Fritz and Robyn Shipley-Gerko: my interest in science manifested as a result of your passion for education. Thank you for your dedication to public service and for nurturing so many students with your support. I dedicate my lifelong commitment to supporting public education to you.

To my colleagues in MCB: I have immense gratitude for the brilliant, passionate scientists with whom I've traveled this journey. Thank you to all of the friends I've made in graduate school, to my cohort of phenomenal classmates, and to Alison and Kayley for the sisterly support you've graciously given.

To the strong women in my life who refuse to back down in the face of systemic adversity, thank you. You have taught me how to maintain strength and poise along the road to progress. I am particularly grateful to the Broad Topics for being a source of balanced inspiration during my graduate studies. Shine Theory forever.

To my roommates that have become dear friends: thank you for your constant support and friendship. In the duration of my graduate studies, I have lived with 18 different people, many of whom have become lifelong friends. Colin, Akemi, Ross, and Allegra, I am particularly lucky to have shared this experience with you.

To Hank and Justin: thank you for encouraging me to start this journey and for your support during the early years of my graduate studies.

To Zach: thank you for helping me find balance and adventure outside of the lab. I appreciate you dearly.

Finally, to the taxpayers of the United States of America: thank you for financially supporting all of this work and my livelihood the past five and a half years. This work was funded by a National Institutes of Health NRSA Trainee appointment on grant number T32 HM 007232 as well as NIH Institute of General Medicine Science grant number R01 GM 031105-33.

Chapter 1

An Introduction to Silent Chromatin and Homologous Recombination in the Budding Yeast *Saccharomyces cerevisiae*

1.1 Introduction to Silent Chromatin in the Budding Yeast *S. cerevisiae*

The budding yeast *Saccharomyces cerevisiae* is a single-celled eukaryote that can mitotically reproduce as both a haploid and diploid organism. To form diploid yeast, two haploid cells of the opposite mating types, **a** and **α**, fuse to create a diploid cell expressing both the **a** and **α** mating-type information. The mating type of haploid cells is determined by the allele present at the *MAT* locus, which contains genes for either the **a** or **α** identity. Copies of both the **a** and **α** genes exist at the *HMR* and *HML* loci, respectively, but are not expressed due to the formation of silent chromatin at these loci. Silencing in yeast is akin to the heterochromatin of plants and animals and has revealed many insights into how repressive chromatin structures execute transcriptional silencing. Silencing of gene expression in *S. cerevisiae* has also been characterized at the telomeres and the rDNA repeats which encode ribosomal RNA (Gottschling *et al.* 1990; Li *et al.* 2017)). However, this study focuses on silent chromatin found at the cryptic mating-type loci *HML* and *HMR*.

1.2 Features of silent chromatin at *HML* and *HMR*

Silencing at *HML* and *HMR* is carried out by the Silent Information Regulator (SIR) proteins (Rine and Herskowitz 1987). DNA sequences called silencers flank both *HML* and *HMR* and recruit proteins important for establishing silencing such as Abf1, Rap1, the Origin Recognition Complex (ORC), and Sir1 (Abraham *et al.* 1984; Feldman *et al.* 1984; Brand *et al.* 1985, 1987; Buchman *et al.* 1988; Kimmerly *et al.* 1988; Mahoney *et al.* 1991; Boscheron *et al.* 1996). The SIR complex, comprising Sir2, Sir3, and Sir4, subsequently binds the silencers and nucleosomes throughout the silenced locus. All 3 members of the SIR complex are required for silencing, whereas Sir1 plays a supportive role in silencing establishment and maintenance (Pillus and Rine 1989; Xu *et al.* 2006; Dodson and Rine 2015). Sir2, the founding member of the highly conserved sirtuin family of deacetylases, removes acetyl marks on histone H4 at position K16 and on histone H3 at positions K9 and K14 across the silenced domain (Imai *et al.* 2000; Landry *et al.* 2000; Smith *et al.* 2000). The absence of particular histone modifications, namely H4K16 hypoacetylation and H3K79 hypomethylation, is a critical feature of silent chromatin (Braunstein *et al.* 1993; Suka *et al.* 2001; Onishi *et al.* 2007; Armache *et al.* 2011). Nucleosomes within *HML* and *HMR* are well positioned, a characteristic not commonly found in actively expressed regions of the genome (Weiss and Simpson 1998; Ravindra *et al.* 1999).

Silent chromatin is a compact structure that offers limited accessibility to many DNA binding proteins. Bacterial DNA methylases and a variety of restriction enzymes are unable to access the DNA sequences embedded within silent chromatin, and the presence of Sir proteins blocks the ability of an endogenous homing endonuclease, HO, to cleave its recognition sequence at *HML* and *HMR* (Connolly *et al.* 1988; Singh and Klar 1992; Gottschling 1992; Loo and Rine 1994). Furthermore, multiple lines of evidence suggest the presence of a higher-order structure of silenced domains relative to euchromatin (Bi and Broach 1997; Cheng *et al.* 1998; Thurtle and Rine 2014).

The stringency of silencing is quite remarkable, as fewer than one in 1,000 wild-type cells lose silencing per round of cell division (Dodson and Rine 2015). Silencing loss in wild-type cells rarely leads to more than one mRNA molecule per cell at steady state, likely a result of the efficiency with which cells can re-establish the silent state. The exact mechanism of silencing by Sir proteins is not completely understood, but involves steric occlusion of some, if not all, of the proteins required for transcription (Sekinger and Gross 2001; Chen and Widom 2005; Steakley and Rine 2015). In the functional competition between silencing machinery and the transcription machinery at *HML* and *HMR*, wild-type cells strongly favor the success of silencing.

The mechanism of inheritance of the silent state remains an active area of research today. The discovery that a *sir1Δ* mutant population comprises cells that faithfully propagate either the silent or unsilent state of expression at *HML* and *HMR* demonstrated the ability of silencing to be epigenetically inherited, thus extending the similarity between yeast silent chromatin and heterochromatin of other organisms (Pillus and Rine 1989; Xu *et al.* 2006). Studies using wild-type cells established a strong dependence on the silencer sequences for trans-generational silencing, yet the specific carrier of silencing information through mitosis remains an enigma (Holmes and Broach 1996; Cheng and Gartenberg 2000).

1.3 Mating-type switching in *S. cerevisiae*

HML and *HMR* exist to facilitate the process of mating-type switching, which has elucidated much of what is known about the repair of double-strand breaks by homologous recombination. In haploid yeast, the homing endonuclease HO is briefly expressed only in mother cells at the end of the G1 stage of the cell cycle (Strathern and Herskowitz 1979). HO makes a double-strand break at the *MAT* locus, while avoiding simultaneous cleavage of the homologous *HML* and *HMR* due to the presence of SIR-mediated silencing at those loci. Homologous recombination leads to gene conversion of the sequence at *MAT*, resulting in a mother-daughter pair of haploid cells with the opposite mating type shortly after completion of cell division. The existence of a cis-acting DNA sequence known as a recombination enhancer (RE) strongly favors repair of *MAT* with the template containing the opposite sequence. The RE is active in *MAT***a** cells, manifesting as a preference to access *HML***α** for recombination after cleavage by HO. In *MAT***α** cells, the RE is inactivated, rendering *HMR***a** the preferred donor for mating-type switching (Wu and Haber 1996).

Double-strand break repair through homologous recombination is an evolutionarily conserved process that requires orchestration of many different proteins and protein complexes. Repair of the double-strand break at *MAT* begins with resection in the 5' to 3' direction on each side of the break (White and Haber 1990; Sun *et al.* 1991). The exposed single strands are bound first by RPA, the functional equivalent of the bacterial single-stranded binding protein (SSB). The recombinase Rad51 then replaces RPA with the help of Rad52, another recombinase

protein, creating a nucleo-protein filament capable of homology search for a suitable repair template (Sugawara *et al.* 2003; Wolner *et al.* 2003; Wang and Haber 2004). Rad51, Rad52, and the ATPase Rad54 facilitate pairing and synapsis of the broken strand with a homologous template sequence. A subset of replication proteins initiates DNA synthesis to fill in the sequence across the break (Lydeard *et al.* 2010).

After synapsis of the Rad51-coated ssDNA with its donor template, homologous recombination can proceed by a variety of mechanisms (reviewed in Paques and Haber 1999). Mating-type switching is a specialized recombination event that occurs only via a type of homologous recombination known as synthesis-dependent strand annealing (SDSA) which results in unidirectional transfer of genetic information from the donor locus, either *HML* or *HMR*, to *MAT* (Haber *et al.* 1980; Klar and Strathern 1984; Ira *et al.* 2006). The nonhomologous portion of the *MAT* sequence that differs from donor template is cleaved off by the Rad1-Rad10 endonuclease, an important step to allow "conservative" replication that only changes the sequence at *MAT* rather than that of *HML* or *HMR* (Fishman-Lobell *et al.* 1992; Lyndaker *et al.* 2008). How exactly mating-type switching is executed exclusively by SDSA over recombination events that involve Holliday junction formation is unclear, although there are known helicases such as Mph1 and Sgs1 that can act to prevent crossovers and thus may contribute to the preference for SDSA (Ira *et al.* 2003; Prakash *et al.* 2009).

1.4 Recombination in the context of heterochromatin

How a process like mating-type switching, and recombination within heterochromatin, affect the chromatin environment at both a double-strand break and its donor locus is an interesting question that probes the interplay of two distinct processes. One of the most well known chromatin changes related to double-strand break repair is the phosphorylation of histone H2A in yeast (or H2Av/H2Ax in other organisms) by the DNA damage checkpoint kinases Mec1 and Tel1 at and surrounding the site of a double-strand break (Shroff *et al* 2004). This formation of gamma-H2A is critical for recruitment of INO80, an ATP-dependent nucleosome-remodeling complex, of which Arp8 is a subunit (Morrison *et al.* 2004). In *arp8Δ* mutant cells, which lack INO80 activity, removal of histone H3 around a double-strand break at *MAT* is slightly impaired (Tsukuda *et al.* 2005). *arp8Δ* mutants also show impaired removal of H2B from *HMR* when it was used as a donor for recombination with *MAT*, suggesting an important role for INO80 nucleosome remodeling activity in chromatin changes at both the site of a double-strand break and its donor locus (Tsukuda *et al.* 2009). Another ATP-dependent nucleosome remodeling complex, SWI/SNF, is implicated in recombination between *MAT* and its heterochromatic donor loci. *In vitro*, SWI/SNF activity is necessary for efficient synapsis between Rad51-coated nucleofilaments and Sir3-bound nucleosomes (Sinha *et al.* 2009). Sir3 and Swi2, the ATPase of the SWI/SNF complex, have a physical interaction that is required for successful synapsis with the same *in vitro* assay (Manning and Peterson 2014), although the *in vivo* role of the SWI/SNF complex in recombination within heterochromatin is unclear.

In addition to molecular studies of chromatin changes during double-strand break repair, chromosome-level dynamics increase after formation of a double-strand break. In *Drosophila* cells, a double-strand breaks that occur within heterochromatin migrates outside of the heterochromatic domain prior to repair in a manner dependent on the Rad51 recombinase (Chiolo *et al.* 2011). Two independent studies in yeast found that inducing a double-strand break at a defined locus greatly increases its mobility within the nucleus, a phenomenon also dependent on Rad51 and Rad54 (Miné-Hattab and Rothstein 2012; Dion and Gasser 2013). While the mechanism of chromosomal movement after a double-strand break is unclear, the ATPase activity of the INO80 chromatin remodeling complex is required for full chromosome mobility, and targeting INO80 to a locus was sufficient to increase its local mobility (Neumann *et al.* 2012).

Whether the process of homologous recombination and its associated chromatin alterations translate to changes in silencing stability at *HML* and *HMR* after mating-type switching was unknown when I started this work. The following study reveals insights into silencing dynamics at *HML* after it serves as a donor locus for homologous recombination.

Chapter 2

The Impact of Homologous Recombination on Silent Chromatin

2.1 Abstract

Specialized chromatin domains repress transcription of genes within them and present a barrier to many DNA-protein interactions. Silent chromatin in the budding yeast *Saccharomyces cerevisiae*, akin to heterochromatin of metazoans and plants, inhibits transcription of PolII- and PolIII-transcribed genes, yet somehow grants access to proteins necessary for DNA transactions like replication and homologous recombination. In this study, I adapted a novel assay to detect even transient changes in the dynamics of transcriptional silencing at *HML* after it served as a template for homologous recombination. Homologous recombination specifically targeted to *HML* via double-strand-break formation at a homologous locus often led to transient loss of transcriptional silencing at *HML*. Interestingly, many cells could template homology-directed repair at *HML* without an obligate loss of silencing, even in recombination events with extensive gene conversion tracts. In the cells that experienced silencing loss following recombination, transcription persisted for two to three hours after all double-strand breaks were repaired. mRNA levels from cells that experienced recombination-induced silencing loss did not approach the amount of mRNA seen in cells lacking transcriptional silencing. Thus, silencing loss at *HML* after homologous recombination was short-lived and limited.

2.2 Introduction

In the budding yeast *Saccharomyces cerevisiae*, the genes at the cryptic mating type loci *HML* and *HMR* are silenced, allowing haploid cells to maintain their identities as either the **a** or **α** mating-type. Yeast silent chromatin shares characteristics with heterochromatin of metazoans and plants, including hypoacetylation of histones (Braunstein *et al.* 1993; Suka *et al.* 2001), epigenetically inherited repression (Pillus and Rine 1989; Xu *et al.* 2006), and compact, higher-order chromatin structure (Bi and Broach 1997; Cheng *et al.* 1998; Weiss and Simpson 1998; Ravindra *et al.* 1999). The Silent Information Regulator (SIR) proteins, Sir1-Sir4, establish silencing via recruitment to regulatory sites called silencers that flank both *HML* and *HMR*. Sir2, the founding member of the highly conserved sirtuin family of protein deacetylases, removes acetyl marks on histone H4 at position K16 and on histone H3 at positions K9 and K14 across the silenced domain (Imai *et al.* 2000; Landry *et al.* 2000; Smith *et al.* 2000). H4K16 deacetylation creates high-affinity binding sites for the Sir complex, comprising Sir2, Sir3, and Sir4, resulting in a chromatin domain that represses transcription of a variety of RNA PolII- and PolIII-transcribed genes (reviewed in Gartenberg and Smith 2016).

Silent chromatin offers limited accessibility to many DNA binding proteins (Singh and Klar 1992; Gottschling 1992; Loo and Rine 1994), yet must allow certain transactions like replication and homologous recombination to occur. In fact, homologous recombination within silent chromatin is a key aspect of yeast biology, as the process of mating-type switching depends upon it (Strathern *et al.* 1982; Kostriken *et al.* 1983). The mating type of haploid yeast is determined by the **a** or α allele present at the *MAT* locus. Un-expressed copies of the *MAT***a** and *MAT*α alleles

reside within silent chromatin at *HML* and *HMR*. Mating-type switching initiates when the HO endonuclease creates a double-strand break at *MAT*, which is then repaired by homologous recombination templated from either *HML* or *HMR*. SIR proteins prevent access of HO to its recognition sequences at *HML* and *HMR*, ensuring that only *MAT* is available for cleavage. Recombination between *MAT* and one of the heterochromatic donor loci results in gene conversion of the sequences at *MAT* from either *HML* or *HMR*.

Mating-type switching in *S. cerevisiae* has provided a foundation for elucidating much of what is known about the repair of double-strand breaks by homologous recombination. Repair of the double-strand break at *MAT* begins with resection in the 5' to 3' direction on each side of the break (White and Haber 1990; Sun *et al.* 1991). The recombinase Rad51 binds the exposed single strands and coordinates with other DNA-repair proteins including Rad54 and Rad52 to facilitate recognition of homologous sequences at either *HML* or *HMR* and carry out strand invasion of the donor locus. Repair of the double-strand break at *MAT* occurs through a type of recombination called synthesis-dependent strand annealing (SDSA), resulting in unidirectional transfer of genetic information from the donor locus, either *HML* or *HMR,* to *MAT* (Haber *et al.* 1980; Klar and Strathern 1984; Ira *et al.* 2006).

Considering the ability of silent chromatin to block DNA-protein interactions and the broad range of proteins needed to repair the cleaved *MAT* locus from the heterochromatic donors, one might expect an obligatory loss of silencing during mating-type switching to allow the recombination machinery access to the silenced template used for repair. To date, there has been no evidence that mating-type switching causes any loss of transcriptional silencing at either *HML* or *HMR*. However, traditional assays of silencing loss that rely on mating phenotypes have limited ability to reveal whether a donor locus becomes expressed as a result of a mating-type switch. In this study, I used a recently developed assay capable of detecting even transient disruptions of silencing (Dodson and Rine 2015) to investigate whether changes to silent chromatin dynamics at the *HML* locus result from its participation in homologous recombination.

2.3 Materials and Methods

Table 2.1: Yeast strains used in this chapter

Name	Genotype	Source
JRY10817	*matΔ::NatMX, lys2, ChrVIII:13192-13237::pseudo-MAT, leu2Δ::pGAL10:HO, HMLα1-INC:α2Δ::cre, hmrΔ::K.l.LEU2, ura3Δ::pGPD:loxP:yEmRFP;tCYC1:KanMX:loxP:yEGFP:tADH1, can1-100, his3-11*	This study
JRY10818	*matΔ::NatMX, lys2, ChrVIII:13192-13237::pseudo-MAT-INC, leu2Δ::pGAL10:HO, HMLα1-INC:α2Δ::cre, hmrΔ::K.l.LEU2, ura3Δ::pGPD:loxP:yEmRFP;tCYC1:KanMX:loxP:yEGFP:tADH1, can1-100, his3-11*	This study
JRY10819	*matΔ::NatMX, lys2, ChrVIII:13192-13237::K.l.URA3-HO, ChrIX:428440::K.l.URA3-HO-INC, leu2Δ::pGAL10:HO, HMLα1ΔHO:α2Δ::cre, hmrΔ::K.l.LEU2, ura3Δ::pGPD:loxP:yEmRFP;tCYC1:KanMX:loxP:yEGFP:tADH, can1-100, his3-11*	This study
JRY10820	*matΔ::NatMX, lys2, swi2Δ::swi2Δ10R, ChrVIII:13192-13237::pseudo-MAT, leu2Δ::pGAL10:HO, HMLα1-INC:α2Δ::cre, hmrΔ::K.l.LEU2, ura3Δ::pGPD:loxP:yEmRFP;tCYC1:KanMX:loxP:yEGFP:tADH1, can1-100, his3-11*	This study
JRY10821	*matΔ::NatMX, dnl4Δ::LYS2, ChrVIII:13192-13237::pseudo-MAT, leu2Δ::pGAL10:HO, HMLα1-INC:α2Δ::cre, hmrΔ::K.l.LEU2, ura3Δ::pGPD:loxP:yEmRFP;tCYC1:KanMX:loxP:yEGFP:tADH1, can1-100, his3-11*	This study
JRY10822	*matΔ::NatMX, lys2, sir3Δ::K.l.URA3, HMLα2Δ::CRE, ura3Δ::pGPD:loxP:yEmRFP;tCYC1:KanMX:loxP:yEGFP:tADH1, can1-100, his3-11, leu2-3,112*	This study
JRY10823	*matΔ::NatMX, lys2, ura3Δ::pGPD:loxP:yEmRFP;tCYC1:KanMX:loxP:yEGFP:tADH1, can1-100, his3-11, leu2-3,112 ;* pJR2538	This study
JRY10824	*matΔ::NatMX, lys2, hmlα2Δ::CRE, ura3Δ::pGPD:loxP:yEmRFP;tCYC1:KanMX:loxP:yEGFP:tADH1, can1-100, his3-11, leu2-3,112 ;* pJR3420, pJR3422	This study
JRY10825	*matΔ::NatMX, lys2, hmlα2Δ::CRE, ura3Δ::pGPD:loxP:yEmRFP;tCYC1:KanMX:loxP:yEGFP:tADH1, can1-100, his3-11, leu2-3,112 ;* pJR3421, pJR3422	This study
JRY10826	*matΔ::NatMX, lys2, ChrVIII:13192-13237::pseudo-MAT, leu2Δ::pGAL10:HO, HMLα2Δ::cre, hmrΔ::K.l.LEU2,*	This study

	ura3Δ::pGPD:loxP:yEmRFP;tCYC1:KanMX:loxP:yEGFP:tADH1-; pJR3422	
JRY10830	*matΔ::NatMX, lys2, arp8Δ::HIS3, ChrVIII:13192-13237::pseudo-MAT, leu2Δ::pGAL10:HO, HMLα1-INC:α2Δ::cre, hmrΔ::K.l.LEU2, ura3Δ::pGPD:loxP:yEmRFP;tCYC1:KanMX:loxP:yEGFP:tADH1, can1-100, his3-11*	This study
	K.l., Kluyveromyces lactis	

All strains in this study were derived from strain JRY9628 (Dodson and Rine 2015), which is derived from W303 (R. Rothstein, Columbia University). Deletion of *HMR* was accomplished via one-step integration (Gueldener *et al.* 2002) of the *Kluyveromyces lactis (K. lactis) LEU2* gene using the *hmrΔ::K.lac.LEU2* forward/reverse primers and confirmed with sequencing. *pGAL10:HO* (Herskowitz and Jensen 1991) was integrated at the *LEU2* locus with the *leu2Δ::pGAL10:HO* forward/reverse primers.

To create the *SNP-INC* at *HML::cre*, site-directed mutagenesis was performed on the *HML::cre* sequence from JRY9628 using the *HML-INC* forward/reverse primers. To construct the pseudo-*MAT* locus, two rounds of site-directed mutagenesis were performed on the *HML::cre* sequence from JRY9628 using the *SNP-R* forward/reverse primers and the *SNP-L* forward/reverse primers. The pseudo-*MAT* locus was inserted between the *YHL045W* and *YHL044W* open reading frames on the left arm of ChrVIII, replacing the sequences between base-pairs 13,192 and 13,237, using the *ChrVIII::pseudo-MAT* forward/reverse primers. For strain JRY10818, the *HML::cre* sequence with *SNP-INC* was inserted at the same location on ChrVIII with the *ChrVIII::pseudo-MAT* forward/reverse primers.

To remove the endogenous HO recognition sequence from *HML::cre* in strain JRY10819, Gibson assembly (Gibson *et al.* 2009) was performed with two overlapping fragments of *HML::cre* from JRY9628 using primers *ΔHO-5'* and *ΔHO-3'* in a way that deleted base-pairs 356-475 of the *α1* sequence, leaving *α1* with base-pairs 1-355;476-528 intact.

To insert the HO recognition sequence into the *K. lactis URA3* sequence, a 3-step Gibson assembly was performed that inserted base-pairs 377-465 of the *α1* sequence between base-pairs 200 and 201 of the *K. lactis URA3* sequence using primers *K.lac.URA3-HO-5'* and *K.lac.URA3-HO-3'*. The *K.lacURA3-HO* construct was then inserted at the same position on the left arm of ChrVIII as pseudo-*MAT* in JRY10817 with the *ChrVIII::K.lac.URA3-HO* forward/reverse primers.

To insert the *K. lactis URA3* sequence containing the HO recognition sequence with

SNP-INC and *SNP-R* onto ChrIX, a 3-step Gibson assembly was performed that inserted base-pairs 377-465 of the *α1* sequence containing *SNP-INC* and *SNP-R* between base-pairs 200 and 201 of the *K. lactis URA3* sequence using primers *K.lac.URA3-HO-5'* and *K.lac.URA3-HO-3'*. This construct was then inserted on the right arm of ChrIX in between base-pairs 428,440 and 428,441 with the *ChrIX::K.lac.URA3-HO-INC-SNPR* forward/reverse primers.

To insert the *swi2Δ10R* allele into the *SWI2* locus, a sequence to create a guide RNA to target cleavage of *SWI2* by Cas9 (Jinek *et al.* 2012) was first cloned into the BsmBI sites of pYTK050 (M.E. Lee *et al.* 2015) using the *SWI2-sgRNA* forward/reverse primers. The full guide RNA sequence was excised from this plasmid and inserted into the BsaI sites of pWCD2257 (Dueber laboratory, UC-Berkeley, described in figures S5B of M. E. Lee et al. 2015), which contains the Cas9 sequence on a yeast *CEN/ARS* plasmid, thus creating pJR3417. pJR3417 was then transformed into JRY10817 alongside a portion of *swi2Δ10R* from CP1413 (Manning and Peterson 2014) that was PCR-amplified using the *swi2Δ10R* forward/reverse primers to create strain JRy10820. Successful replacement of *SWI2* by *swi2Δ10R* was confirmed by sequencing of the *SWI2* locus.

All genomic positions described are from the S288C reference genome version R64-2-1 (Engel et al. 2013), which can be accessed at http://downloads.yeastgenome.org/sequence/S288C_reference/genome_releases/.

All strains are available upon request.

Table 2.2: Plasmids used in this chapter

Name	Description	Source
pJR2538	*pGAL1:cre HIS3 ampR CEN/ARS*	Goldstein, A.L. et al., Yeast (1999)
pJR3420	*creΔNΔC_HOcutsite URA3 ampR CEN/ARS*	This study
pJR3421	*creΔNΔC URA3 ampR CEN/ARS*	This study
pJR3422	*pGAL10:HO HIS3 ampR CEN/ARS*	This study

To create the *creΔNΔC* construct, the first 20 base-pairs and final 167 base-pairs were omitted from the *cre* ORF. To create the *creΔNΔC_HOcutsite* construct, a 57 base-pair sequence encompassing the last 23 base-pairs of the *Yalpha* sequence and the first 34 base-pairs of the *Zalpha* sequence that spans the HO recognition sequence was inserted between base-pairs 336 and 337 of the *creΔNΔCΔ* sequence.

Table 2.3: Oligonucleotides used in this chapter

Name	Sequence
leu2Δ::pGAL10:HO	GTCTAAGGCGCCTGATTCAAGAAATATCTTGACCGCAGTTCCG

forward	AGATCAAAAATCATCGC
leu2Δ::pGAL10:HO reverse	TAAAGTTTATGTACAAATATCATAAAAAAAGAGAATCTTTTG GCGTATTACTACTCCAGC
HML-INC forward	GGGACTACTTCGCACAACAGTATAATTT
HML-INC reverse	AAATTATACTGTTGTGCGAAGTAGTCCC
hmrΔ::K.lac.LEU2 forward	ATATCATACAAGAAGAAAATAGTTGCAAATCTCTAACCCAGCT GTGAAGATCCCAGCAAA
hmrΔ::K.lac.LEU2 reverse	ACACAGTATAATGATAACACATTGGTAGTGTGACTACTAGAAC CGGAACCTGTATTATTT
SNP-R forward	TACAAAACCAAAACCAGGGTTGATAAAATTATACTGTTGCGCG
SNP-R reverse	CGCGCAACAGTATAATTTTATCAACCCTGGTTTTGGTTTTGTA
SNP-L forward	AATTTGCCTGCATTACCTGTCGATGCAACGAGTG
SNP-L reverse	CACTCGTTGCATCGACAGGTAATGCAGGCAAATT
ChrVIII::pseudo-MAT forward	CATCGCTATATTCATGGTGACGGCTCATCTCTAAAGCTTCGTC AAACACCCAACAAAGCA
ChrVIII::pseudo-MAT reverse	TTCTTTCGTCAACATACTAAAGCACGCTATCGGAGACTTCTGA CCAGAGTCATCCTTAGC
ΔHO-5′	ATATCCGTCACCACGTACTTGCAGAGAAGACAAGACATTT
ΔHO-3′	AAATGTCTTGTCTTCTCTGCAAGTACGTGGTGACGGATAT
K.lac.URA3-HO-5′	ATTCCGTGCTGCATTTTGTCCATCCAAGATATCAACGTGTG
K.lac.URA3-HO-3′	TTGTAGAGTGGTTGACGAATATTTCAGTTATGAGGGTACTGT
ChrVIII::K.lac.URA3-HO forward	CATCGCTATATTCATGGTGACGGCTCATCTCTAAAGCTTCGTT TTATTTAGGTTCTATCGAGGAGAAAAAG
ChrVIII::K.lac.URA3-HO reverse	TTCTTTCGTCAACATACTAAAGCACGCTATCGGAGACTTCAAG ATGAAGTTGAAGTGAGTGTTGC
ChrIX::K.lac.URA3-HO-INC-SNPR forward	CTTCACATTTTCACGCAATATCTTCAACAGAATTTGAAGGGTT TTATTTAGGTTCTATCGAGGAGAAAAAG
ChrIX::K.lac.URA3-HO-INC-SNPR reverse	TAAAAGCAAAATAAACAGAGTTATCCAGATATGAGATTGTAA GATGAAGTTGAAGTGAGTGTTGC
SWI2-sgRNA forward	GACTTTTTAAAGGTTCGCCAAATGAG
SWI2-sgRNA reverse	AAACCTCATTTGGCGAACCTTTAAAA
swi2Δ10R forward	TGTTTACTGCCGAGCAATCC
swi2Δ10R reverse	GCTTCTTGTTCCTCCGATGTAG
HO-α1 probe forward	AGATAAGGGTATAGCCATATGAGTG
HO-α1 probe reverse	CCTGTTCCTTCCTCTCGATTT
K.lac.URA3-HO probe forward	CACTCCCGTCAATTAGTTGC
K.lac.URA3-HO probe reverse	CAATACCAGCACCAGTAACCC
pseudo-MAT-amplify forward	GTTGAGTTCAGTTTGTAGCAGT

pseudo-MAT-amplify reverse	GGACAGAAATAAGTATGTTGCATAACTT
pseudo-MAT-seq-A	CAGAAAAGAGCAGTGAAAGATTTC
pseudo-MAT-seq-B	GATCCTGGCAATTTCGGCTA
cre-3'-RTPCR forward	TTCCAGCAGGCGCACCATTG
cre-3'-RTPCR reverse	GTCTGGACACAGTGCCCGTG
ACT1-RTPCR forward	TGTCCTTGTACTCTTCCGGT
ACT1-RTPCR reverse	CCGGCCAAATCGATTCTCAA

Galactose induction of double-strand breaks

Strains were grown at 30°C in liquid Complete Supplement Mixture (CSM) -Trp (Sunrise Science Products, San Diego, CA) with raffinose (2% W/V) as a carbon source and containing G418 to select for an un-rearranged LoxP reporter cassette, then diluted into liquid CSM -Trp medium with raffinose and allowed to grow to an A600 of 0.2-0.4. Cultures were then split and received either galactose or raffinose to a final concentration of 2%. For experiments with a glucose recovery, cultures were centrifuged at 4,000rpm for 15 minutes, then re-suspended in CSM -Trp medium containing glucose (2% W/V) and allowed to keep growing. For each time point, a sample of culture was diluted in CSM -Trp with glucose and plated onto CSM -Trp glucose plates.

Colony imaging and silencing loss analysis

Colonies were grown for 5-7 days on CSM-Trp glucose plates and then imaged with a Zeiss Axio Zoom.V16 microscope equipped with ZEN software (Zeiss, Jena, Germany), a Zeiss AxioCam MRm camera and a PlanApo Z 0.5× objective. Sectoring patterns were scored manually. Colonies that were at least one-quarter green were counted as "early silencing loss" events. Red colonies with wild-type levels of sectoring were scored as colonies that "maintained silencing". Colonies that were petite or with morphologies suggestive of reciprocal crossover leading to a dicentric chromosome were omitted from analysis.

DNA blots

DNA hybridization blots were performed as previously described with only minor changes (Southern 2006). Probes were radiolabeled by random priming with P^{32}-αdCTP using either the Amersham Rediprime II Random Primer Labeling System (GE Healthcare) or the Amersham Megaprime DNA Labeling System (GE Healthcare). Membranes were exposed 16-72 hours with a Storage Phosphor Screen (GE Healthcare) and imaged with a Typhoon Trio (GE Healthcare). To determine the ratio of pseudo-*MAT* molecules cut, the intensity of each pseudo-*MAT* band was quantified using the Gel Analysis function of ImageJ software (NIH, Bethesda, MD). Ratios were calculated by dividing the sum of intensities of the two cut pseudo-*MAT* bands by the sum of intensities of the cut and uncut pseudo-*MAT* bands.

For blots probing the pseudo-*MAT* and *HML::cre* loci (Figures 2.1C, 2.5C, 2.6B, and 2.7B) DNA was digested with XbaI and PacI. The probe comprised a 505 base-pair sequence centered around the HO recognition sequence that was amplified from the *HML::cre* sequence of JRY10817 using the *HO-α1 probe* forward/reverse primers.

For blots probing the *URA3-HO* sequences (Figure 2.3B), DNA was digested with PacI and PvuII. The probe comprised a 501 base-pair sequence surrounding the HO recognition sequence that was amplified from the *K. lactis URA3-HO* sequence of JRY10819 using the *K.lac.URA3-HO probe* forward/reverse primers.

For blots probing the *creΔNΔC_HOcutsite* sequences (Figure 2.10D), DNA was digested with KpnI and SacI. The probe comprised a 298 base-pair sequence centered around the HO recognition sequence in pJR3420 that was amplified using primers with the sequences CGTATATCCTGGCAGCGGT and CGCGGTCTGGCAGTAAAAA.

RNA Preparation and quantitative RT-PCR

RNA was extracted from cells using the hot-acid-phenol method (DOI: 10.1002/0471143030.cb2703s54). 10ug of RNA was digested with DNase I (Invitrogen, Carlsbad, CA) then purified with phenol-chloroform extraction followed by precipitation with 100% ethanol and 0.3M sodium acetate, pH 5.2. cDNA was synthesized from 2ug of DNAse-treated RNA with the SuperScript III First-Strand Synthesis System for RT-PCR (Invitrogen, Carlsbad, CA) and oligo(dT) primers. Quantitative PCR of cDNA was executed to detect the 3' end of the *cre* transcript specific to *HML::cre* with the *cre-3'-RTPCR* forward/reverse primers using the Thermo Scientific DyNAmo HS SYBR Green qPCR Kit (Fisher Scientific, Chicago, IL) and a Mx3000P machine (Stratagene, acquired by Agilent Technologies, Santa Clara, CA). Expression levels were normalized first to *ACT1* mRNA, which was measured using the *ACT1-RTPCR* forward/reverse primers, and then to *cre* mRNA levels from strain JRY10822. Samples were analyzed in technical triplicate.

Calculating gene conversion frequencies

For colony genotyping, colonies were re-suspended in 200uL TE buffer and 100uL of glass beads. 200uL of 25:24:1 phenol:chloroform:isoamyl alcohol was added, and tubes were subjected to two rounds of 20-second bead-beating using a FastPrep-24 (MP Biomedicals, Santa Ana, CA). Tubes were centrifuged for 10 minutes at 15,000 rpm, and 1 uL of the aqueous phase was removed for PCR. PCR amplification of the pseudo-*MAT* locus on ChrVIII was carried out using the *pseudo-MAT-amplify* forward/reverse primers and Phusion High-Fidelity DNA polymerase (New England Biolabs, Ipswich, MA). A PCR cleanup reaction was performed using Agencourt AMPure XP reagent and the Beckman NX automated liquid handler by UC Berkeley DNA Sequencing Facility, and PCR were products sequenced with primers *pseudo-MAT-seq-A* and *pseudo-MAT-seq-B*. Sequencing traces were analyzed using SnapGene software (from GSL Biotech; available at snapgene.com). For each of the 3

differentiating SNPs, sequencing traces that showed peaks of both the original pseudo-*MAT* sequence and the sequence at *HML::cre* were scored as partial gene conversions and those that showed only the *HML::cre* sequence were scored as full gene conversions. Multiple negative-control samples in the sequencing process with no template DNA failed to produce PCR amplicons for sequencing, indicating that the presence of both alleles within a single colony reflected heterogeneity of genotype within the colony rather than cross-contamination of sequencing samples.

Measuring half-life of *cre* mRNA

Strain JRY10823, bearing the plasmid pJR2538 with *pGAL:cre*, was grown to saturation in CSM-His with galactose medium, then diluted to an O.D. of 0.25 in the same medium and grown to an OD of 0.5. At this point, a pre-induction sample was removed. The culture was centrifuged for 10 minutes at 4,000 RPM and resuspended in CSM-His with glucose to turn off *cre* expression. A time 0 sample was immediately taken, and samples were taken every 10 minutes for the first 60 minutes and then every 15 minutes for the next 60 minutes. RNA extraction and quantitative-RT-PCR were performed as described above.

2.4 Results

2.4.1 Design of a pseudo-*MAT* locus to test stability of gene silencing at a heterochromatic donor locus

To ask whether silencing stability is affected by homologous recombination within the silenced domain, I created a strain that allowed temporal control of homology-directed repair of a double-strand break at a custom-designed locus using *HML* as a donor. To monitor silencing stability, I employed an assay previously developed by our lab called the Cre-Reported Altered States of Heterochromatin, or CRASH, assay (Dodson and Rine 2015). In this assay, the *cre* recombinase gene replaces the native *α2* sequence at *HML.* Loss of silencing at *HML::cre* leads to the production of Cre protein, which then acts on a reporter cassette with loxP sites positioned around *RFP* and *GFP* genes such that Cre-mediated recombination creates a permanent and heritable switch in fluorescence from red to green and a loss in resistance to the drug G418 [Figure 2.1A].

In mating-type interconversion, a double-strand break at *MAT* results in transposition of the sequence from the *HML* donor locus to the *MAT* locus where it is then expressed. Hence, transposition of *cre* from *HML* to *MAT* would cause all cells to switch from *RFP* expression to *GFP* expression, rendering the CRASH assay ineffective. To induce a double-strand break that would be repaired by recombination targeted to *HML::cre* yet circumvent this problem, I constructed a pseudo-*MAT* locus on the left arm of ChrVIII [Figure 2.1B]. This pseudo-*MAT* locus consisted of a 2.4kb region of *HML::cre*, omitting the silencers as well as the 3' end of the *cre* ORF which encodes the protein's active site required for Cre function. The lack

of these sequences and flanking homology guaranteed that repair of the double-strand break at the pseudo-*MAT* locus could not restore a functional *cre* gene at that locus. The endogenous recognition sequence of the HO endonuclease found within the *α1* ORF served as a target for double-strand break induction at the pseudo-*MAT* locus. The *HO* gene under control of the *GAL10* promoter allowed temporal regulation of double-strand break induction by addition of galactose to the growth medium. Under physiological conditions of *HO* expression, Sir proteins prevent access of HO to its recognition sequence at *HML,* but *HO* overexpression can lead to low levels of *HML* cleavage (Connolly, White, and Haber 1988, K. Sieverman and J. Rine, unpublished results). To ensure that HO caused double-strand break formation only at the pseudo-*MAT* locus and not at *HML::cre* itself, I mutated the *α1* sequence at *HML::cre* to contain a single-nucleotide polymorphism (SNP) that eliminates HO's ability to cleave it, historically known as *MATα-inc* (Nickoloff *et al.* 1990) but called SNP-INC here. To further distinguish the homologous sequences at *HML::cre* and pseudo-*MAT*, I added two SNPs to the pseudo-*MAT* locus on either side of the HO cleavage site: one within the *cre* sequence, called SNP-L, and one to the right of the HO recognition sequence, called SNP-R. I also deleted the *MAT* and *HMR* loci in this strain to prevent cleavage by HO at its recognition sequence within them.

The pseudo-*MAT* locus was inserted 13kbp from the end of the left arm of ChrVIII. I chose this location to encourage efficient recombination between *HML::cre* and pseudo-*MAT* based upon two considerations: recombination efficiency correlates with contact frequency, as measured by Hi-C (C. S. Lee *et al.* 2015), and with similarity in chromosomal arm length (Agmon *et al.* 2013). Mating-type switching involves only nonreciprocal recombination. To allow us to focus exclusively on the outcomes of nonreciprocal events, the orientation of *HML::cre* and pseudo-*MAT* was such that reciprocal recombination via crossover would create a dicentric chromosomal fusion. Such events can be recognized by the slow growth and abnormal colony morphology resulting from various resolutions of the dicentric chromosome. Focusing our analysis on colonies with typical morphology allowed us to evaluate only non-reciprocal recombination events that would not lead to *cre* expression from the pseudo-*MAT* locus. Upon induction of *HO* in this strain (JRY10817) double-strand breaks were evident within 30 minutes, with breaks persisting but reduced after 4 hours of *HO* expression [Figure 2.1C].

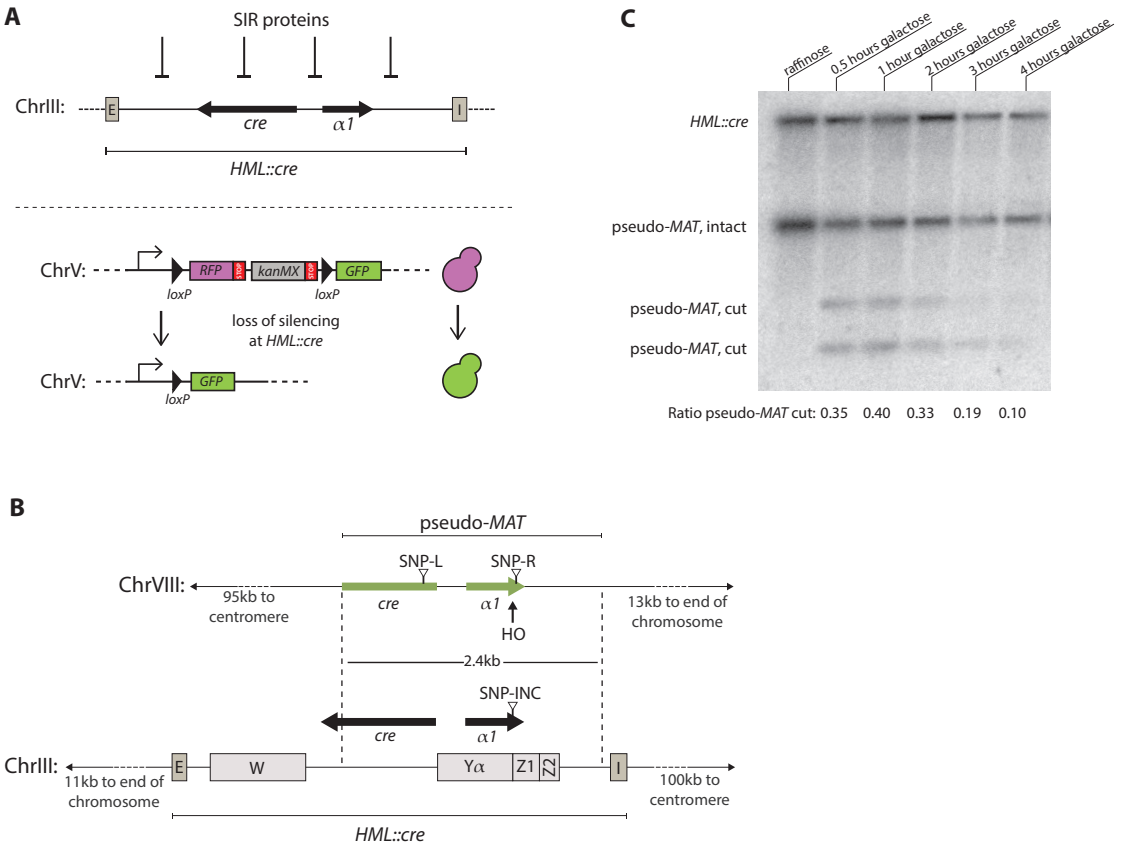

Figure 2.1 (A) Diagram of the CRASH (Cre-Reported Altered States of Heterochromatin) assay used to measure transcriptional silencing stability at *HML.* (B) Schematic for directing homologous recombination between *HML::cre* and pseudo-*MAT* in strain JRY10817. The region between the dashed lines represents the 2.4kb sequence of *HML::cre* that was inserted onto the left arm of chromosome VIII. The first 844 base-pairs of the *cre* ORF were included, omitting the protein's active-site sequences. The sequence on chromosome VIII in green indicates that it is transcribed whereas the homologous sequences in black at *HML::cre* sequence are silenced. The open triangles represent three SNPs that distinguish the homologous regions: two SNPs on chromosome VIII on either side of the site of the HO-induced double-strand break, SNP-L and SNP-R, and one SNP within *HML* that destroys the HO recognition sequence, SNP-INC. SNP-L is located 45 base-pairs into the *cre* ORF, 721 base-pairs from the site of HO cleavage, and SNP-R is at the 20th base-pair of the Z region, approximately 16 base-pairs away from the site of the double-strand break. The arrow indicates the site of HO cleavage. (C) DNA-hybridization blot of double-strand break kinetics in JRY10817. A blot evaluating *HML::cre* and pseudo-*MAT* showed double-strand break induction at pseudo-*MAT* after *HO* induction for the times shown. Here and in subsequent figures, the ratio of cut:total pseudo-*MAT* band

intensities were calculated using densitometry, as described in Materials and Methods.

2.4.2 Homology-directed repair decreased the stability of silencing at the donor locus

Induction of *HO* and subsequent plating on solid medium lacking galactose yielded colonies in which at least one-quarter of cells had switched from *RFP* to *GFP* expression, indicating a silencing loss event early in colony growth. Moreover, there was a clear trend of increasing silencing loss events with increasing duration of *HO* induction [Figure 2.2A]. A subculture incubated in non-inducing (raffinose) medium yielded primarily red colonies, indicating that without exposure to galactose, the stability of silencing at *HML::cre* was unaffected.

To determine whether the loss in silencing stability upon *HO* induction resulted from the presence of HO itself rather than from the resulting double-strand break, I created a strain identical to the assay strain but also harboring SNP-INC at pseudo-*MAT* (JRY10818), thus lacking any recognition sequence for HO to cleave. In this strain, induction of *HO* resulted in no discernable increased likelihood of silencing loss [Figure 2.2B]. Hence, destabilization of silencing at *HML::cre* depended on double-strand-break formation at the pseudo-*MAT* locus rather than growth in galactose medium or some yet-unrecognized ability of HO to influence silencing loss.

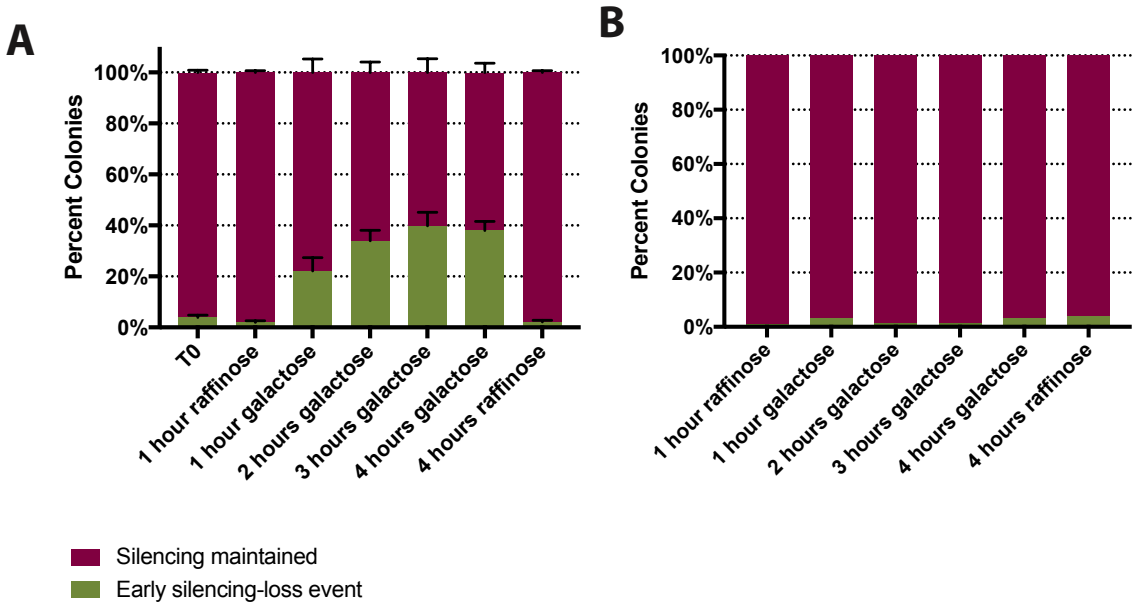

Figure 2.2 Silencing loss after *HO* induction by galactose. (A) Increased likelihood of silencing loss after *HO* induction and double-strand breaks at pseudo-*MAT* in JRY10817. (B) JRY10818, which harbors the SNP-INC allele at both *HML::cre* and pseudo-*MAT,* did not show increased likelihood of silencing loss after *HO* induction. As a negative control in both experiments, part of the culture was maintained in raffinose. Here and in subsequent figures, early silencing loss events were defined as colonies that were at least one-quarter green, indicating a silencing loss event by the 4-cell stage of the colony. A minimum of 300 colonies (A) or 175 colonies (B) was analyzed for each time point. The means and standard deviations of three independent biological replicates are shown in panel (A).

To investigate whether recombination involving *HML::cre* itself was required for the increase in silencing-loss events or whether repair of a double-strand break anywhere in the genome would cause silencing instability, I induced HO cleavage at a locus whose template for homology-directed repair was not *HML::cre.* Specifically, an HO recognition sequence was engineered into a *URA3* gene at the same position on ChrVIII as pseudo-*MAT*, with an uncleavable version of the same *URA3* construct inserted on ChrIX [Figure 2.3A]. As expected, *HO* induction in this strain (JRY10819) resulted in double-strand-break formation on ChrVIII with cleavage levels similar to those seen at pseudo-*MAT* [Figure 2.3B]. Even in colonies grown from cells with the longest induction times, there was no increase in silencing loss at *HML::cre* [Figure 2.3C]. Thus, the silencing instability induced at *HML::cre* after cleavage of ChrVIII required a double-strand break in a sequence homologous to *HML::cre.*

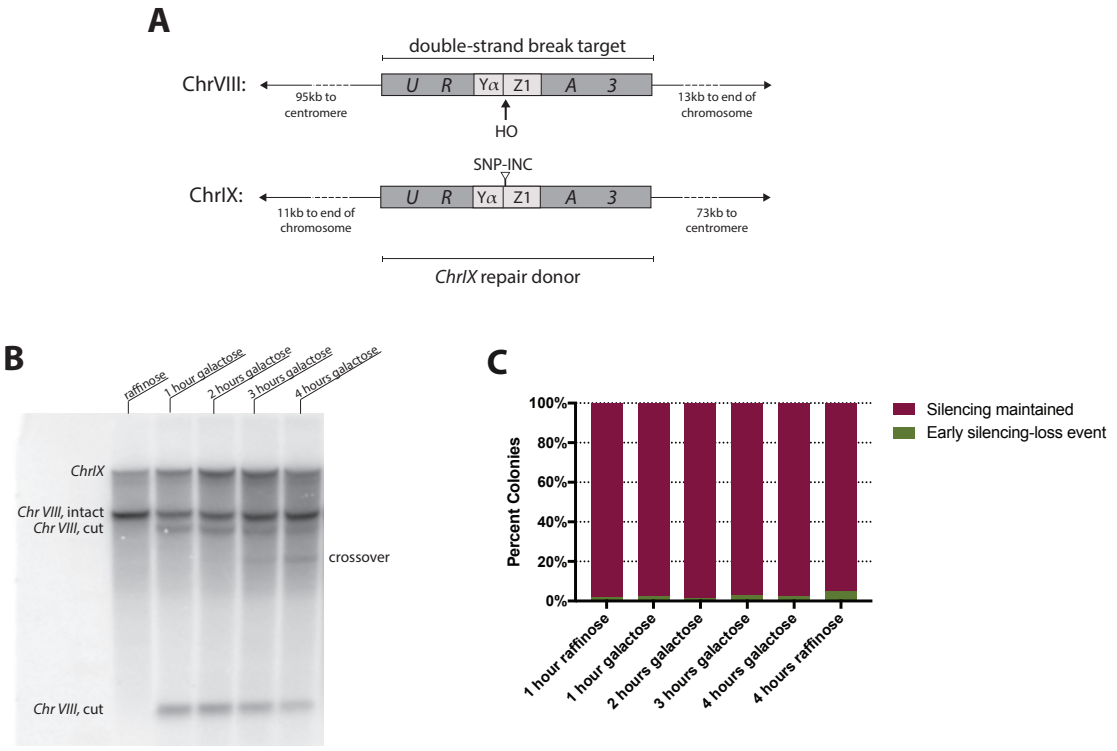

Figure 2.3 Recombination elsewhere in the genome did not increase likelihood of silencing loss. (A) Schematic for directing homologous recombination between ChrVIII and ChrIX in strain JRY10819. An 89 base-pair sequence of the Yalpha-Z1 regions spanning the HO recognition sequence from *MATα* was inserted into the *K. lactis URA3* gene, which was placed at the same place on ChrVIII where the pseudo-*MAT* locus resided. The same sequence was copied onto ChrIX with the SNP-INC substitution that prevented HO from cleaving ChrIX. Additionally, the HO recognition sequence was deleted from *HML::cre,* thus directing all HO-mediated double-strand breaks to ChrVIII and inducing homology-directed repair off of ChrIX. The arrow indicates the site of HO cleavage. (B) DNA-hybridization blot of double-strand-break induction kinetics in JRY10819. A blot evaluating the *URA3-HO* construct on ChrVIII and *URA3-HO-INC* on ChrIX showed double-strand-break induction at *URA3-HO* after *HO* induction for the times shown. A band indicative of a reciprocal crossover between ChrVIII and ChrIX appeared after 3 hours of *HO* induction. (C) HO cleavage leading to recombination events between ChrVIII and ChrIX did not increase the likelihood of silencing loss at *HML::cre*. As a negative control, part of the culture was maintained in raffinose. A minimum of 400 colonies was analyzed for each time point.

2.4.3 Gene conversion of SNPs at pseudo-*MAT* was diagnostic of recombination with *HML::cre*

In mating-type interconversion, homologous recombination via synthesis-dependent strand annealing (SDSA) results in gene conversion of the double-strand break recipient sequence to that of its donor locus. I analyzed the DNA sequence at pseudo-*MAT* for evidence of gene conversion of the 3 SNPs differentiating it from *HML::cre* in colonies grown on solid medium lacking galactose after HO induction. After a 1-hour HO induction, 42% of the resultant colonies showed evidence of gene conversion at the pseudo-*MAT* locus of at least one of the three SNPs [Figure 2.4A]. After 4 hours of HO induction, 72% of colonies exhibited gene conversion [Figure 2.4B], exceeding the fraction that lost silencing, as discussed more thoroughly below.

The SNP-INC was most likely to gene convert: approximately 39% of colonies showed appearance of the SNP-INC sequence now in the pseudo-*MAT* locus after 1 hour of HO induction and 66% after 4 hours of induction. SNP-L and SNP-R were less likely to gene convert: approximately 26% of colonies showed gene conversion at SNP-L and 29% at SNP-R after a 1-hour induction. Many colonies showed only partial gene conversion of any given SNP, meaning that both the original pseudo-*MAT* and the *HML::cre* sequences were detected at the pseudo-*MAT* locus within the DNA from a single colony. This genotypic heterogeneity is discussed further below.

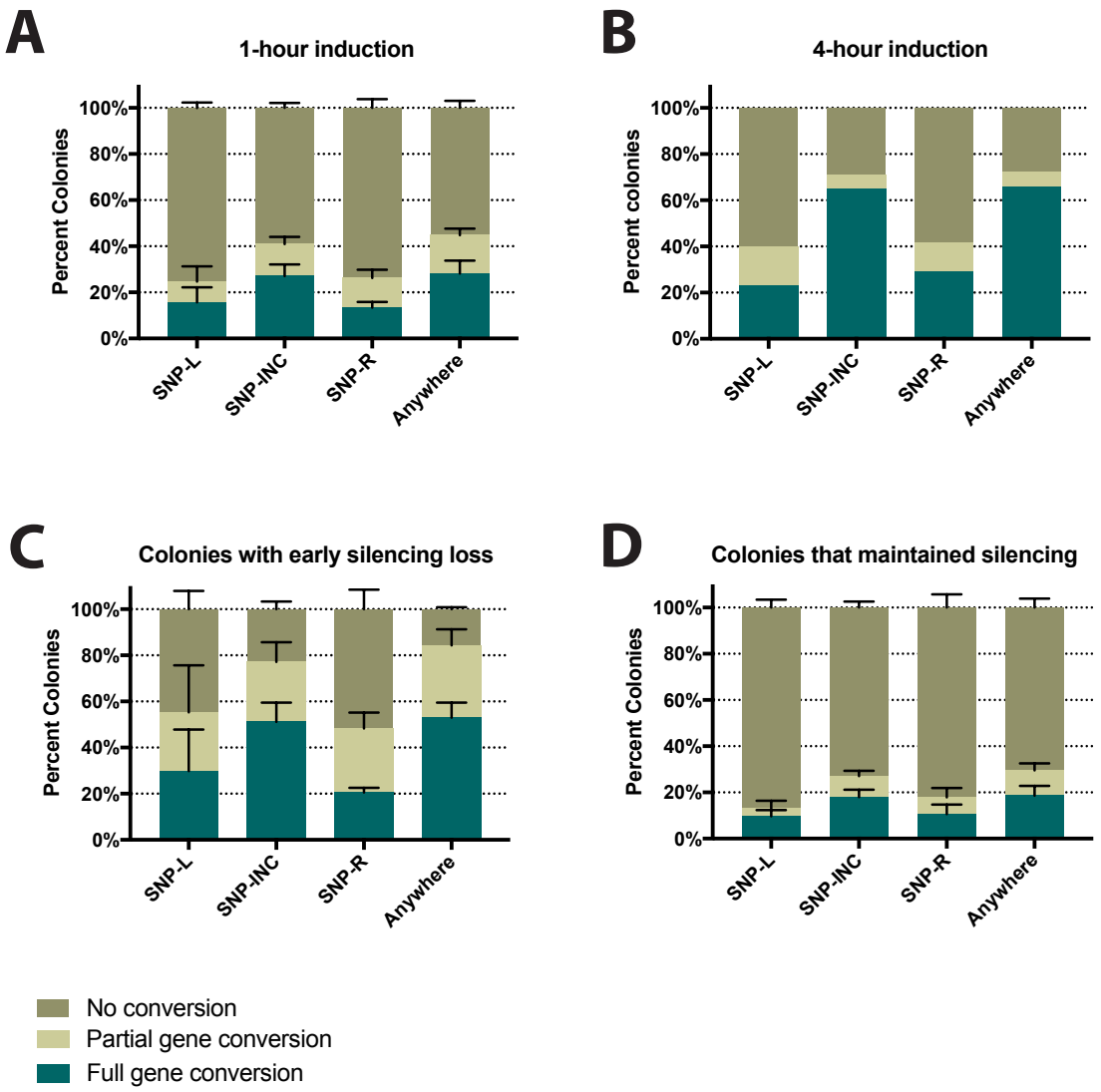

Figure 2.4 Gene conversion frequencies at pseudo-*MAT* after (A) 1-hour *HO* induction and (B) 4-hour *HO* induction. In panels C and D, gene conversion frequencies are shown after a 1-hour *HO* induction in colonies that (C) experienced an early silencing-loss event or (D) maintained silencing. For each of the 3 SNPs distinguishing pseudo-*MAT* and *HML::cre*, the percentage of colonies that showed evidence of gene conversion is shown. Gene conversion events were scored as full gene conversion events if I detected only presence of the *HML::cre* sequence and partial events if I detected both the *HML::cre* and pseudo-*MAT* sequences within a single colony. Sequences from 142 colonies (A), 169 colonies (B), 31 colonies (C), and 111 colonies (D) are represented in these data. The means and standard deviations of three independent biological replicates are shown in panels (A), (C), and (D).

2.4.4 Recombination could occur without silencing loss

Inducing recombination between pseudo-*MAT* and *HML::cre* led to a population of cells that experienced a greater likelihood of silencing loss, yet many cells gave rise to red colonies that had maintained silencing after 4 hours of *HO* expression. The DNA blot [Figure 2.1C] suggested that not all recipient loci had been cleaved at any time point, but that analysis could not distinguish between molecules that had been cut and repaired and molecules that had never received a double-strand break. Additionally, 34% of colonies showed no evidence of gene conversion after 4 hours of *HO* induction. Therefore, it was possible that colonies that maintained silencing arose from cells that did not experience a double-strand break and subsequent recombination between pseudo-*MAT* and *HML::cre*. Alternatively, some cells may have managed to execute homology-directed repair from *HML::cre* with no impact on silencing stability.

To distinguish these two possibilities, I analyzed gene conversion frequencies from colonies that were either red or at least one-quarter green to ask whether gene conversion was evident in both populations. After a 1-hour *HO* induction, approximately 84% of colonies that lost silencing early in colony growth exhibited gene conversion at pseudo-*MAT* [Figure 2.4C], demonstrating a strong correlation between recombination with *HML::cre* and silencing instability. Interestingly, approximately 30% of red colonies, which maintained silencing through multiple rounds of cell division, also showed evidence of gene conversion [Figure 2.4D]. Therefore, homologous recombination between pseudo-*MAT* and *HML::cre* did not lead to an obligate loss of silencing.

Conceivably, silencing might be maintained only in cells with short conversion tracts, while those with extensive gene conversion may lose silencing stability. However, gene conversion into the *cre* sequence at SNP-L, 721 base-pairs from the HO cleavage site, was possible without subsequent transcriptional activation of the *cre* gene at *HML*, as evidenced by the approximately 16% of colonies that maintained silencing yet experienced gene conversion at SNP-L [Figure 2.4D].

2.4.5 Kinetics and extent of silencing loss

To investigate how quickly silencing loss at *HML::cre* appeared after *HO* induction and how long it persisted after homology-directed repair, I monitored mRNA levels of the *cre* transcript specific to *HML::cre* before, during, and after a 1-hour *HO* induction. I calculated the half-life of *cre* mRNA to be approximately 3 minutes after glucose shutoff of a *cre* gene being driven by the *pGAL1* promoter [Figure 2.5A]. Thus, measurements of *cre* mRNA by RT-qPCR closely reflected the real-time transcriptional output of cells. Prior to double-strand break induction, *cre* mRNA levels were approximately 9,000-fold lower than those in a *sir3Δ* strain lacking transcriptional silencing at *HML::cre* [Figure 2.5B]. After a one-hour induction of *HO*, *cre* mRNA levels increased approximately 10-fold. *Cre* expression peaked at nearly 100-fold higher than pre-double-strand break induction 2 hours after

quenching *HO* expression, at which time all double-strand breaks at pseudo-*MAT* appeared to be repaired [Figure 2.5D]. Five hours after quenching *HO* expression, *cre* mRNA levels had returned to approximately 10-fold higher levels than before double-strand break induction [Figure 2.5B], suggesting that many cells that had lost silencing had restored it by this time and were no longer producing *cre* transcripts. In strain JRY10818 harboring the SNP-INC at pseudo-*MAT*, expressing *HO* did not cause an increase in *cre* transcript levels, indicating that the increase in *cre* transcripts was specific to cultures experiencing the double-strand break at the pseudo-*MAT* locus [Figure 2.5C].

To estimate the extent of silencing loss resulting from homologous recombination, I compared the number of colonies that experienced silencing loss before, during, and after a 1-hour *HO* induction to the *cre* mRNA levels measured by RT-qPCR. Prior to *HO* induction, approximately 2% of cells gave rise to colonies with an early silencing loss event [Figure 2.5E]. After a one-hour *HO* induction, approximately 23% of resultant colonies experienced an early silencing loss event. The percentage of colonies with silencing loss remained similar after a 2-hour quench of *HO* expression with glucose, suggesting that no additional cells lost silencing during that time. The highest levels of *cre* expression were seen at the 2-hour quench time, at which point they were about 1% that of a *sir3Δ* population [Figure 2.5B]. Assuming that the population of cells that experienced silencing loss re-established silencing with similar kinetics, I inferred that 23% of the population expressed *cre* at a maximum of 1% of full de-repression, as measured in mRNA from the entire population. Therefore, the cells that lost silencing after homologous recombination within *HML::cre* expressed *cre* at much lower levels per cell than did fully de-repressed cells.

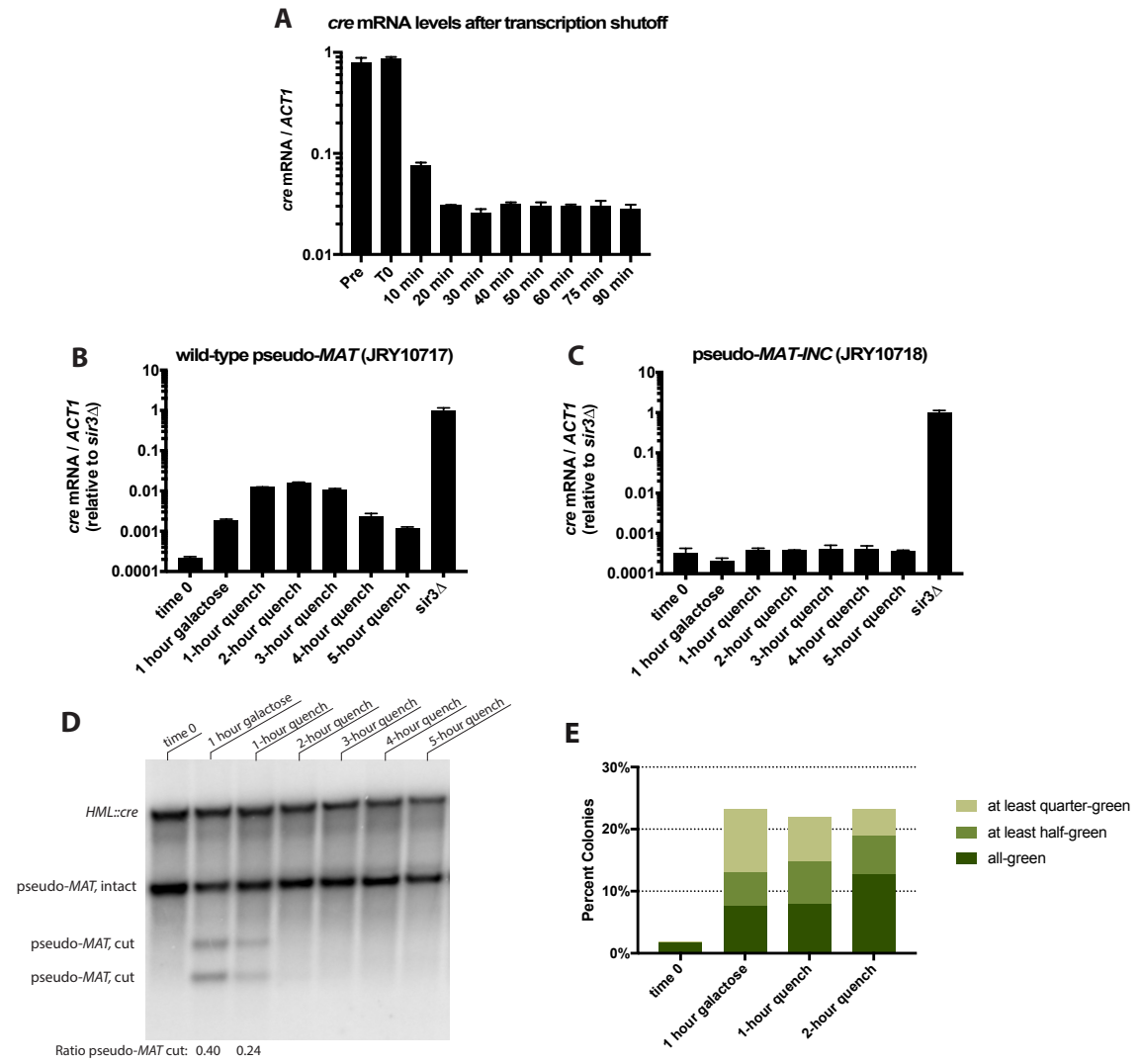

Figure 2.5 (A) Kinetics of *cre* mRNA stability after glucose-mediated shutoff of p*GAL1:cre.* (B and C) qRT-PCR quantification of *cre* mRNA in (B) a strain with a cleavable pseudo-*MAT* locus (JRY10817) and (C) strain without a cleavable pseudo-*MAT* locus (JRY10818) before and after a 1-hour *HO* induction and subsequent quench with glucose. *Cre* mRNA levels were normalized to *ACT1* mRNA levels and all data points are relative to *cre* mRNA levels of a *sir3Δ* strain (JRY10822), which lacks transcriptional silencing. Data represent the means and standard deviations of three technical replicates. (D) DNA-hybridization blot of double-strand break formation and repair kinetics. A blot evaluating *HML::cre* and pseudo-*MAT* showed double-strand break induction at pseudo-*MAT* after a 1-hour *HO* induction and subsequent quench with glucose. (E) Percentage of colonies that were all-green, at least half-green but not all-green, or at least one-quarter green but not half-green during the

qRT-PCR time course. Data shown are the means of two independent biological replicates.

2.4.6 The absence of functional SWI/SNF and INO80 complexes did not influence silent chromatin dynamics during or after homologous recombination

Previous studies indicate that the presence of Sir3, one of the structural components of silent chromatin, prevents an early step of homologous recombination (Sinha *et al.* 2009). The nucleosome remodeling activity of the SWI/SNF complex is required *in vitro* for successful synapsis between Rad51-coated filaments and Sir3-bound nucleosomal donors. *SWI2* encodes the ATPase of the SWI/SNF complex and interacts directly with Sir3 *in vitro* (Manning and Peterson 2014). An allele of *SWI2*, *swi2Δ10R*, lacks sequences necessary for Swi2's interaction with Sir3 and eliminates the ability of the SWI/SNF complex to facilitate pairing between Rad51-coated filaments and Sir3-coated nucleosomal donors *in vitro* (Manning and Peterson 2014). Although *swi2Δ10R* is not reported to inhibit recombination between *MAT* and *HMR* *in vivo* (Manning and Peterson 2014), I hypothesized that the stability of silenced chromatin during recombination may be affected in this mutant.

The INO80 complex is recruited to sites of double-strand breaks (Morrison *et al.* 2004) and plays a role in removal of nucleosomes at *HMR* during mating-type switching (Tsukuda *et al.* 2009). Although some subunits of the INO80 complex are essential for viability, *arp8Δ* mutants lack the ATP-dependent nucleosome remodeling activity of the INO80 complex but are viable. Hence, I hypothesized that the propensity of silencing loss after homologous recombination could be altered in an *arp8Δ* background.

I repeated the *HO* induction time course in a *swi2Δ10R* mutant (JRY10820) that was otherwise isogenic with the wild-type assay strain. Levels of silencing instability after 1 and 2 hours of *HO* induction appeared slightly higher than in the *SWI2* parent strain, though the background level of silencing instability was also slightly higher [Figure 2.6A], suggesting no increased likelihood of silencing loss in the *swi2Δ10R* mutant after *HO* induction. There was no obvious difference in the overall recombination frequency between pseudo-*MAT* and *HML::cre* or the kinetics of break induction and repair in the *swi2Δ10R* mutant relative to wild type [Figures 2.6B and 2.6C].

DNA double-strand break formation and repair at pseudo-*MAT* also led to silencing loss in an *arp8Δ* mutant [Figure 2.7A]. The extent of silencing loss appeared slightly lower than in wild-type colonies, although additional replicates are needed to determine whether this difference is significant. The kinetics of break formation and repair were unchanged in *arp8Δ* cells [Figure 2.7B], nor was there an obvious different in overall recombination frequency as measured by gene conversion [Figure

2.7C].

Gene conversion frequencies in colonies that maintained silencing and in colonies that had early silencing loss were not markedly different from wild type in either mutant [Figures 2.6D-E and 2.7 D-E], suggesting that the mutant *swi2Δ10R* allele and absence of functional INO80 complex had little if any effect on the ability of the cleaved pseudo-*MAT* locus to participate in homologous recombination. The fraction of colonies that experienced an early silencing-loss event, with or without gene conversion, appeared slightly elevated in a *swi2Δ10R* background relative to wild type [Figures 2.7 A-D]. However, wild-type and *swi2Δ10R* colonies that showed evidence of gene conversion had similar likelihoods of experiencing early silencing loss relative to colonies that did not show evidence of gene conversion [Figure 2.7G]. Thus, the presence of the mutant *swi2Δ10R* allele did not largely influence the likelihood of whether the *HML::cre* locus lost silencing when it participated in homologous recombination. Conversely, the fraction of colonies that experienced early silencing-loss events, with or without gene conversion, appeared slightly lower in the *arp8Δ* background relative to wild type [Figures 2.7E-F]. However, as with *swi2Δ10R*, the fold increase in silencing-loss events in colonies that experienced gene conversion was indistinguishable from wild type [Figure 2.7G]. Therefore, the propensity to lose silencing after homologous recombination was not greatly influenced by INO80 activity.

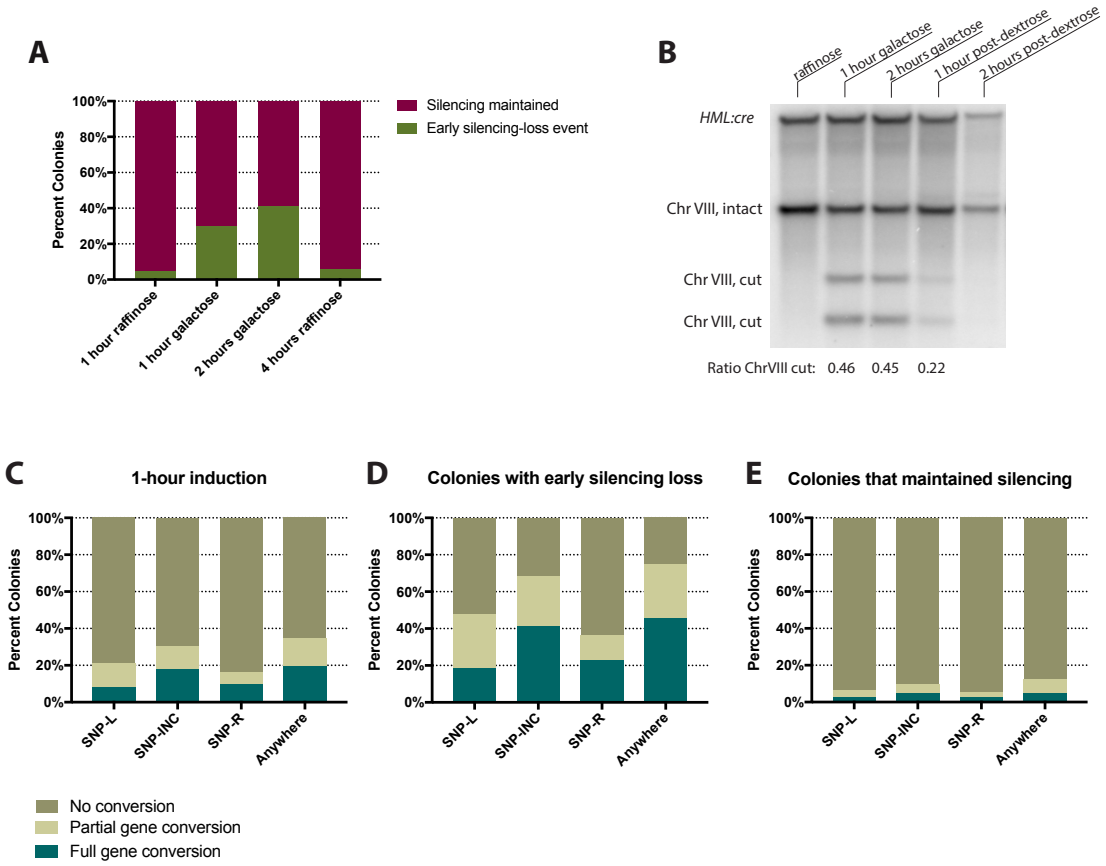

Figure 2.6 (A) As in wild type, *HO* induction increased likelihood of silencing loss in a *swi2Δ10R* mutant (JRY10820). Early silencing-loss events were defined as in previous figures. A minimum of 460 colonies was analyzed for each time point. (B) A DNA-hybridization blot evaluating *HML::cre* and pseudo-*MAT* showed double-strand-break induction at pseudo-*MAT* after *HO* induction in *swi2Δ10R* (JRY10820) for the times shown. (C-E) Gene conversion frequencies in *swi2Δ10R* at pseudo-*MAT* after 1-hour *HO* induction in (C) all colonies, and in (D) colonies that experienced an early silencing-loss event or (E) maintained silencing. For each of the 3 SNPs distinguishing pseudo-*MAT* and *HML::cre*, the percentage of colonies that showed evidence of gene conversion is shown. Gene conversion events were scored as in previous figures. Sequences from 125 colonies (C), 44 colonies (D), and 81 colonies (D) are represented in these data.

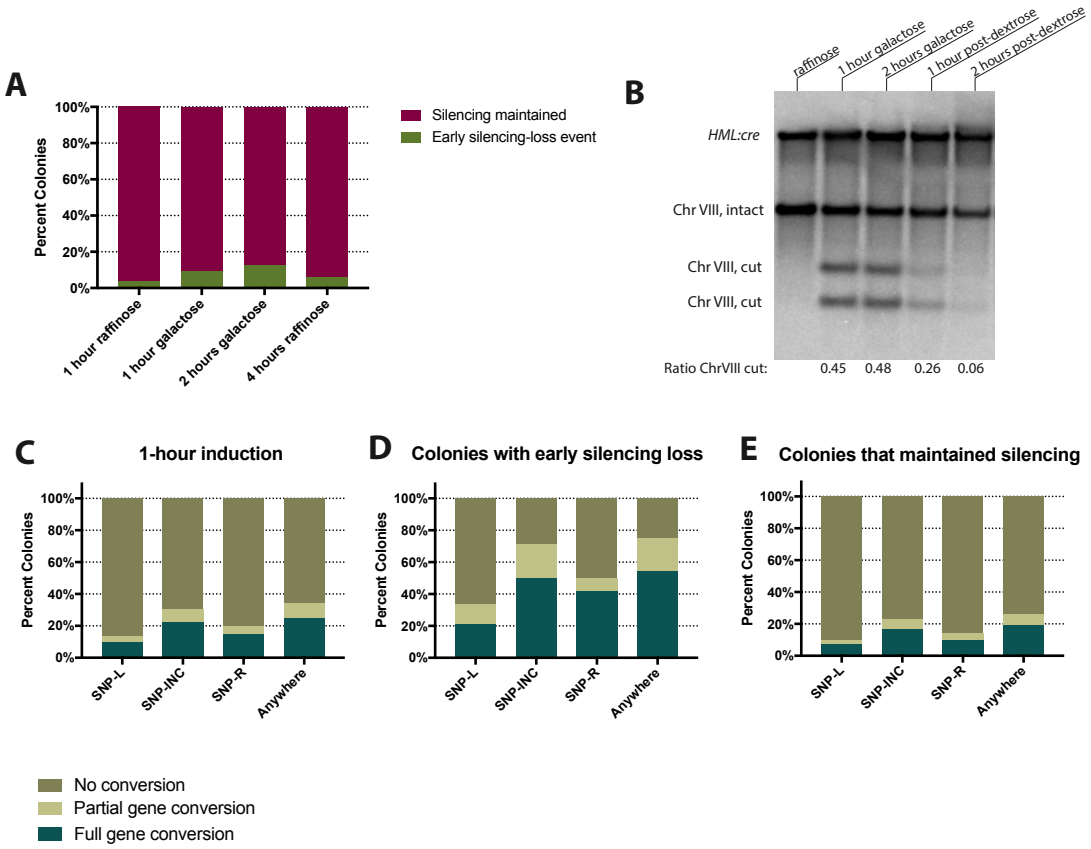

Figure 2.7 (A) Silencing loss in an *arp8Δ* mutant (JRY10830) after induction of *HO*. Early silencing-loss events were defined as in previous figures. A minimum of 583 colonies was analyzed for each time point. (B) A DNA-hybridization blot evaluating *HML::cre* and pseudo-*MAT* showed double-strand-break induction at pseudo-*MAT* after *HO* induction in *arp8Δ* (JRY10830) for the times shown. (C-E) Gene conversion frequencies in *arp8Δ* at pseudo-*MAT* after 1-hour *HO* induction in (C) all colonies, and in (D) colonies that experienced an early silencing-loss event or (E) maintained silencing. For each of the 3 SNPs distinguishing pseudo-*MAT* and *HML::cre*, the percentage of colonies that showed evidence of gene conversion is shown. Gene conversion events were scored as in previous figures. Sequences from 151 colonies (C), 24 colonies (D), and 127 colonies (D) are represented in these data.

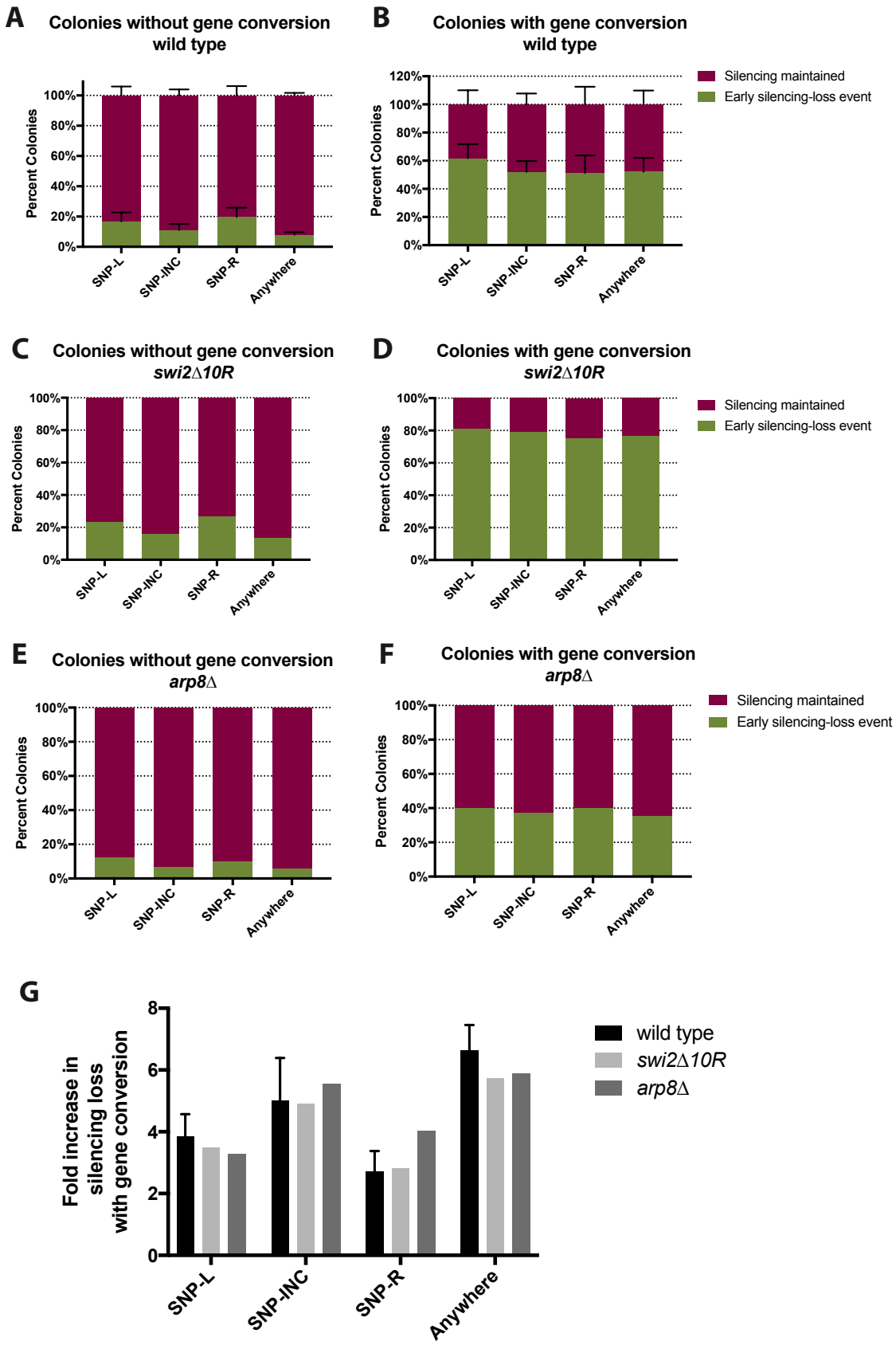
A
Colonies without gene conversion
wild type
Percent Colonies
100%
80%
60%
40%
20%
0%
SNP-L
SNP-INC
SNP-R
Anywhere
B
Colonies with gene conversion
wild type
120%
Silencing maintained
Early silencing-loss event
C
Colonies without gene conversion
swi2Δ10R
D
Colonies with gene conversion
swi2Δ10R
E
Colonies without gene conversion
arp8Δ
F
Colonies with gene conversion
arp8Δ
G
Fold increase in silencing loss with gene conversion
8
6
4
2
0
wild type
swi2Δ10R
arp8Δ

Figure 2.8 Frequencies of early silencing loss events after a 1-hour *HO* induction in in wild-type colonies (JRY10817) that (A) did not exhibit gene conversion and (B) exhibited at least partial gene conversion, *swi2Δ10R* colonies (JRY10820) that (C) did not exhibit gene conversion and (D) exhibited at least partial gene conversion, and *arp8Δ* colonies (JRY10830) that (E) did not exhibit gene conversion and (F) exhibited at least partial gene conversion at each of the 3 SNPs distinguishing pseudo-*MAT* and *HML::cre*. Partial gene conversion events were scored as in Figures 2.4 and 2.6. The means and standard deviations of three independent biological replicates are shown in (A) and (B). (G) Fold increase in percentage of colonies that showed an early silencing loss event with evidence of gene conversion relative to no gene conversion. The means and standard deviations of three biological replicates are shown for wild-type colonies.

2.4.7 Investigating causes of genotypic heterogeneity within colonies

As mentioned earlier, I observed some partial gene conversion events at the pseudo-*MAT* locus, whereby both the original pseudo-*MAT* and *HML::cre* sequences were detected within a single colony after *HO* induction. This genetic heterogeneity suggested that not all cells within the colony experienced the same molecular outcome at the pseudo-*MAT* locus after double-strand break induction. Double-strand breaks can be repaired independently of homologous recombination by non-homologous end joining (NHEJ), and breaks made by HO often lack a sequence scar when repaired by NHEJ (Kramer *et al.* 1994; Moore and Haber 1996; Haber 2012). I hypothesized that the genotypic heterogeneity observed within colonies might be a result of post-replication breaks in which one chromatid of ChrVIII underwent homology-directed repair at pseudo-*MAT* while the other was non-homologously end joined, leading to two different repair outcomes and thus two genotypes within the colony. To test this, I deleted the DNA ligase IV gene, *DNL4,* which is required for NHEJ (Wilson *et al.* 1997), in the parental strain used for all of the experiments above. In this mutant (JRY10821), I did not observe a marked difference in likelihood of silencing loss upon HO induction [Figure 2.9A], overall gene conversion frequencies after a one-hour induction, or the frequency of partial gene conversions relative to full gene conversions [Figure 2.9B]. Thus, repair through NHEJ was not a major contribution to removal of double-strand breaks and did not account for the genotypic heterogeneity within colonies.

Yeast cells sometimes fail to separate fully after completing a round of cell division. To determine whether the genotypic heterogeneity within colonies might have resulted from incomplete separation of single cells at the time of plating, leading to colonies with more than one original founder cell, I used a micromanipulator to separate single cells after 1 hour of *HO* induction onto solid medium, thus ensuring that the resultant colonies were progeny of one cell. Sequencing results from these colonies showed that the appearance of partial gene conversion events persisted [Figure 2.9C], though at a lower frequency. Thus, differences in sequence at the

pseudo-*MAT* locus existed between founder cells and their progeny, and incomplete separation of cells after division likely contributed to some of the genetic heterogeneity seen within colonies that were plated by traditional bead-based spreading.

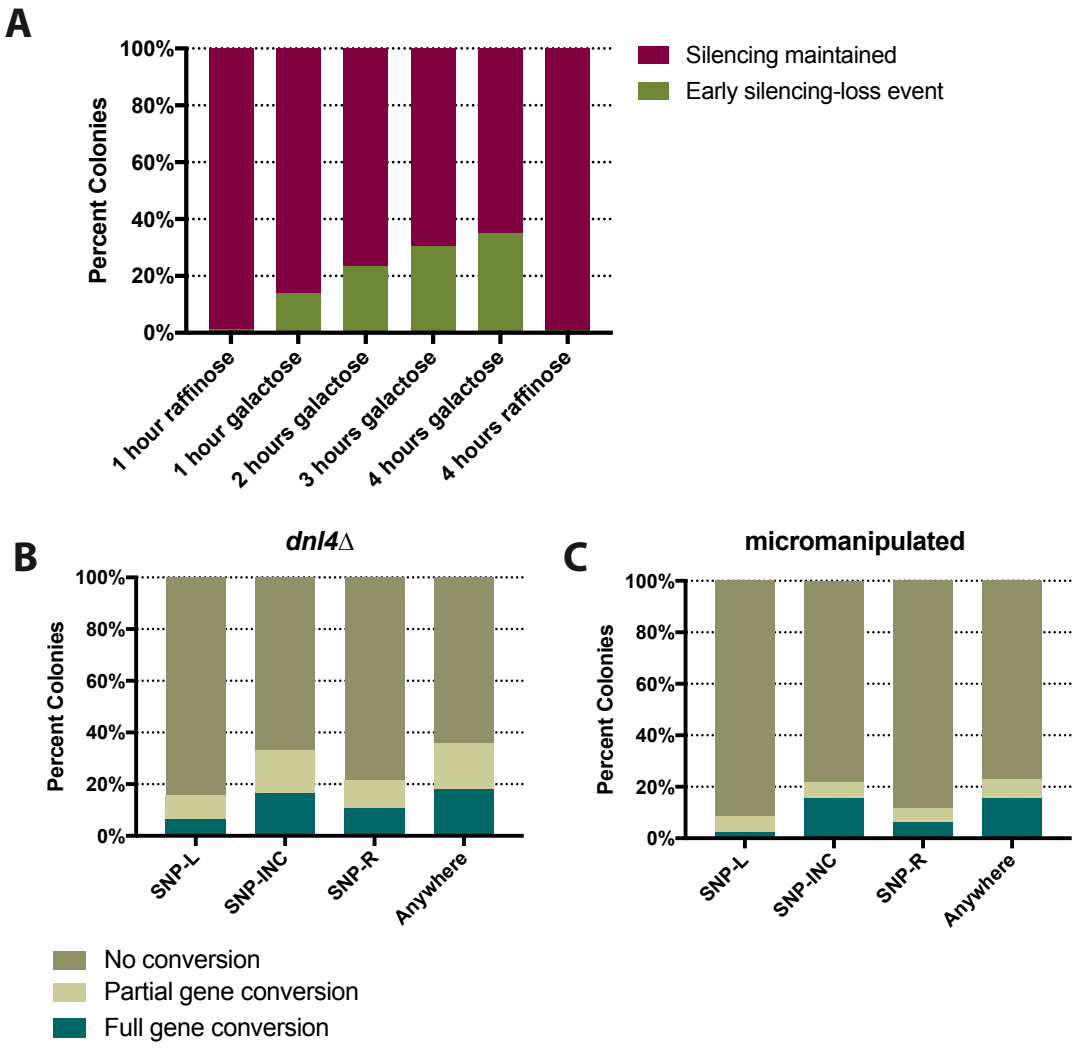

Figure 2.9 (A) As in wild type, *HO* induction increased likelihood of silencing loss in a *dnl4Δ* mutant (JRY10821). Early silencing-loss events were defined as in Figures 2 and 3. A minimum of 218 colonies was analyzed for each time point. Gene conversion frequencies at pseudo-*MAT* after a 1-hour *HO* induction in (B) a *dnl4Δ* mutant (JRY10821) or (C) wild-type cells (JRY10817) that were micromanipulated to ensure only one founder cell per colony. For each of the 3 SNPs distinguishing pseudo-*MAT* and *HML::cre*, the percentage of colonies that showed evidence of gene conversion is shown. Sequences from 140 colonies (B) and 97 colonies (C) are represented in these

data.

2.4.8 Lessons learned from initial assay designs

Developing the recombination assay used in these experiments proceeded through early designs that yielded unexpected biological insights. In one of the earliest assay designs for inducing recombination at *HML::cre*, I inserted a truncated *cre* sequence, *creΔNΔC,* onto a *CEN-ARS* plasmid with 57 base-pairs of the HO recognition sequence, thus creating pJR3420 [Figure 2.10A]. As a negative control, I generated a plasmid with the same truncated *cre* sequence but lacking the HO recognition sequence (pJR3421). I created strains bearing either of these plasmids under uracil selection and an additional *CEN-ARS* plasmid containing *pGAL10:HO* under histidine selection. Thus, induction of *HO* by addition of galactose would make a double-strand break in the strain bearing pJR3420 but not pJR3421, and subsequently direct homologous recombination to *HML::cre* to repair the broken plasmid.

Upon galactose induction, I found that both strains continued to divide [Figure 2.10B] and give rise to viable colonies [Figure 2.10C], but the strain with pJR3420 had a massive reduction in viability on –Ura selection medium. DNA-hybridization blot analysis showed that upon receiving the HO-mediated double-strand break, pJR3420 was subsequently lost rather than repaired [Figure 2.10D]. Thus, recombination between pJR3420 and *HML::cre* was not sufficiently efficient to serve as an assay for investigating the effects of homologous recombination on silencing at *HML::cre*.

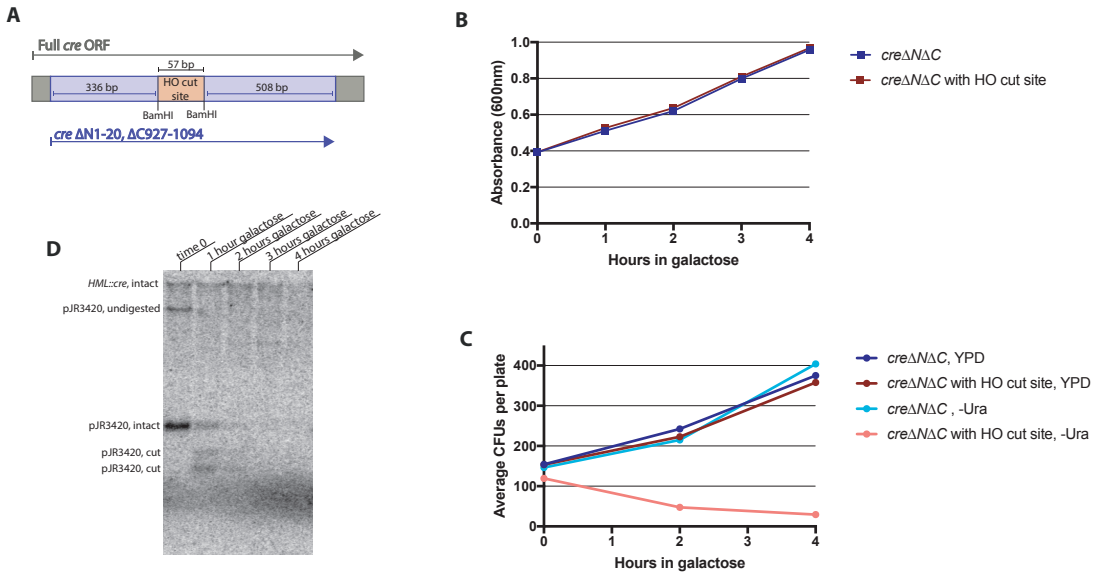

Figure 2.10 (A) Schematic of the truncated *cre* sequence, *creΔNΔC*, with a 57 base-pair insertion of the HO recognition sequence in pJR3420. The first 20 and last 167 base-pairs of the *cre* ORF were excluded in the *creΔNΔC* construct. (B) Growth after addition of galactose as measured by absorbance at 600nm for a strain bearing pJR3420 (*creΔNΔC* with HO cut site) and pJR3421 (*creΔNΔC* alone) (C) Viability after addition of galactose of strains bearing either pJR3420 or pJR3421 on non-selective YPD medium and –Ura medium for plasmid selection. (D) A DNA-hybridization blot evaluating the *cre* sequence found in *HML::cre* and pJR3420 showed double-strand break formation within and subsequent loss of pJR3420.

In our initial attempt to induce recombination at *HML::cre* by creating a break at pseudo-*MAT*, I did not engineer the *INC* allele into *HML::cre* [Figure 2.11A]. Induction of *HO* after addition of galactose in strain JRY10826 led to cutting at *HML::cre* after 2 hours of *HO* expression [Figure 2.11B]. The ability of HO to access its recognition sequence at a Sir-silenced locus after over-expression of *HO* has been reported in the past (Connolly *et al.* 1988).

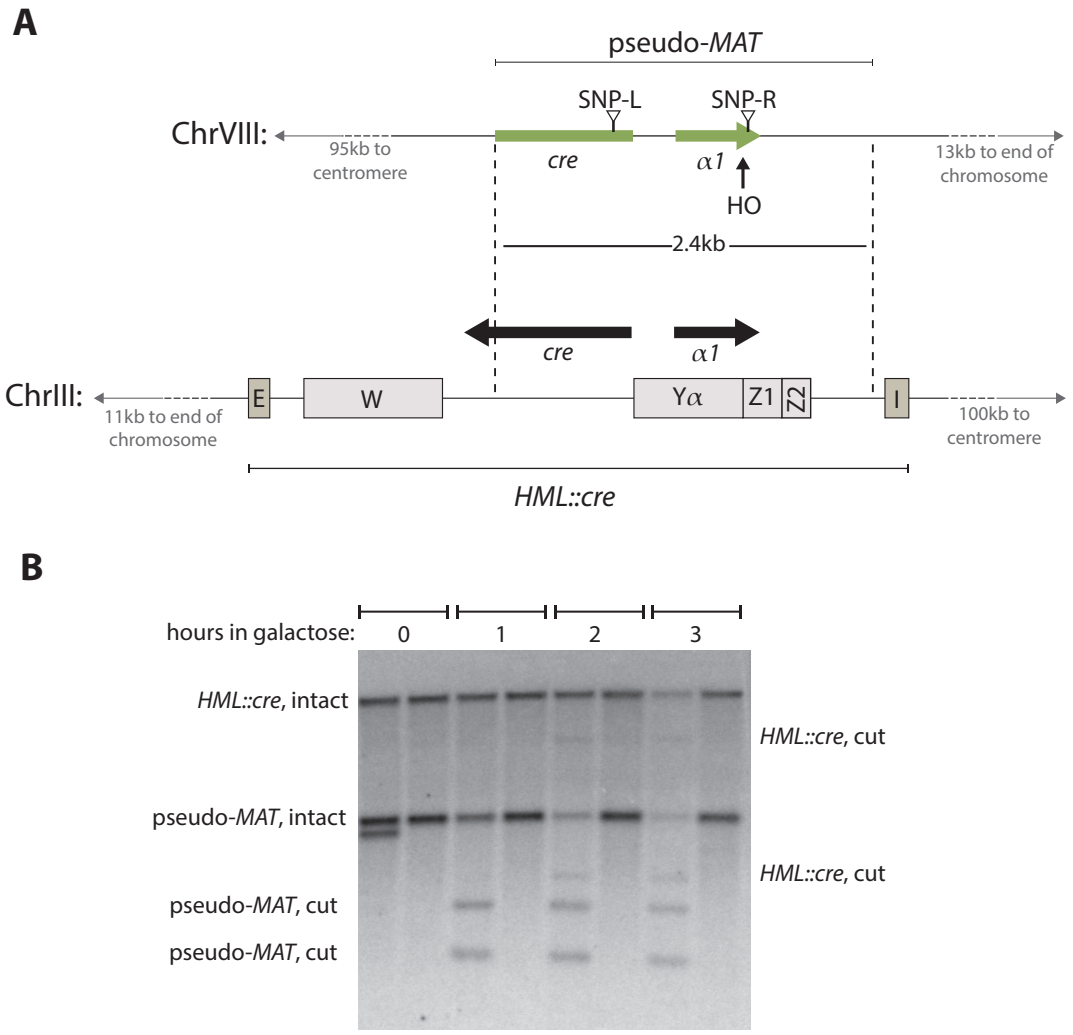

Figure 2.11 (A) Schematic of pseudo-*MAT* and *HML::cre* without the *INC* allele at *HML::cre* in strain JRY10826. (B) A DNA-hybridization blot evaluating *HML::cre* and pseudo-*MAT* showed double-strand break induction at *HML::cre* after *HO* induction for 2 hours.

2.5 Discussion

In this study, I developed an assay to test the consequences of homologous recombination within silent chromatin on the stability of gene silencing. I used the *HO* endonuclease gene under control of the *GAL10* promoter to temporally control double-strand break induction at pseudo-*MAT*, a locus that shared homology with *HML::cre*. I found that double-strand-break repair templated from *HML::cre* increased the frequency of silencing loss events, although recombination was possible without disruptions to silencing even in repair events with extensive gene conversion tracts. Recombination-induced expression from *HML::cre* was rapid and lasted on the order

of hours before silencing was re-established. Double-strand break induction and silencing loss outcomes were not greatly affected in either a *swi2Δ10R* mutant or a *dnl4Δ* mutant. Founder cells and their progeny did not always share the same sequence at the pseudo-*MAT* locus after gene conversion, leading to genetic heterogeneity within some colonies.

2.5.1 Silencing loss often, but not always, accompanied homologous recombination

After induction of *HO*, many cells gave rise to colonies that had lost silencing in at least one cell by the four-cell stage of growth, resulting in colonies that were at least one-quarter green. This increase in silencing-loss events was specific to strains in which a double-strand break was repaired from *HML::cre*, as homologous recombination not involving *HML::cre* did not change the likelihood that it would lose silencing. In approximately one-third of colonies that did not lose silencing after one hour of *HO* induction, gene conversion occurred at the pseudo-*MAT* locus. Thus, homologous recombination targeted to *HML::cre* led to distinct outcomes where cells either did or did not lose silencing after homology-directed repair.

Why homologous recombination led to silencing loss in some cells but not others remains an interesting puzzle. It was unlikely that the extent of gene conversion tract determined whether silencing was lost, since I found that gene conversion of the distant SNP-L occurred in approximately 16% of colonies that did not lose silencing. In mating-type switching, repair events proceed via a type of homologous recombination known as synthesis-dependent strand annealing (SDSA) (Haber *et al.* 1980; Klar and Strathern 1984; Ira *et al.* 2006), but multiple mechanisms of homologous recombination can repair a double-strand break (reviewed in Pâques and Haber 1997). Perhaps in our assay strain, recombination events between pseudo-*MAT* and *HML::cre* were repaired by different mechanisms of homologous recombination, some of which lead to silencing loss and some of which do not. Mating-type switching is restricted to the end of G1 (Strathern and Herskowitz 1979), whereas our experiments were conducted in cycling cells. Conceivably, the timing of either the double-strand break or the recombination event itself could influence whether or not the *HML::cre* donor locus lost silencing. For example, the sirtuin deacetylase Hst3 is a cell cycle-regulated protein important for maintaining silencing stability at *HML* (Dodson and Rine 2015) and is degraded after S phase but before anaphase (Delgoshaie *et al.* 2014). Finally, it is also possible that the likelihood of silencing loss after recombination reflected stochasticity in the access of the transcription machinery to *HML::cre*.

2.5.2 Silencing loss was transient and limited

I monitored the kinetics and levels of transcripts from *HML::cre* before, during, and after *HO* induction by qRT-PCR. Transcription at *HML::cre* was highest after completion of homologous recombination, perhaps because the presence of repair proteins prevented access of the transcription machinery to the donor locus until

recombination was complete. In the cells that lost silencing, transcription at *HML::cre* resulting from homologous recombination likely did not approach the full level of de-repression. It is unclear whether the green cells contributing to the colonies that were at least one-quarter green but not all-green had lost silencing at the time of plating or whether those silencing loss events occurred post-plating. In the latter scenario, the all-green colonies alone would contribute to the pool of mRNA seen by RT-qPCR within the first few hours. Even so, the increase in all-green colonies seen after *HO* induction to 5-10% of the population would have only given rise to 1% of *cre* mRNA expected with full de-repression, further supporting the conclusion that silencing loss did not approach full de-repression.

Cre mRNA levels had decreased substantially 5 hours after quenching *HO* expression, but were still 9-fold higher than before the induction. A longer time course would presumably show transcriptional silencing returning to its pre-induction levels. Conceivably, some cells within the population may have undergone reciprocal recombination, giving rise to a functional *cre* gene that might not be silenced at the pseudo-*MAT* locus on the resulting dicentric chromosome. Although colonies resulting from such events were excluded from our plating-based analyses, the samples collected for qRT-PCR analysis could include a small percentage cells expressing *cre* from such a restored pseudo-*MAT* locus.

2.5.3 Interactions between Swi2 and Sir3 did not influence silencing stability during homologous recombination

Silent chromatin prevents access of many DNA binding proteins to the sequences within it, and previous studies established a role for ATP-dependent nucleosome remodelers in successful recombination between the *MAT* locus and its heterochromatic donors (Chai *et al.* 2005; Tsukuda *et al.* 2009; Sinha *et al.* 2009). *In vitro*, the SWI/SNF complex is necessary to allow pairing between Rad51-coated filaments and Sir3-coated nucleosomes in an assay that simulates recombination with silent chromatin (Sinha *et al.* 2009). A later study characterized physical interactions between Sir3 and the ATPase subunit of the SWI/SNF complex, Swi2 (Manning and Peterson 2014), as necessary for successful *in vitro* synapsis between Rad-51 filaments and Sir3-coated nucleosomal donors using the same assay. An allele of *SWI2*, *swi2Δ10R*, that abolishes the interaction between Sir3 and SWI/SNF, prevents *in vitro* pairing of Rad51-filaments with Sir3-bound nucleosomes. Nevertheless, I found no substantial differences between the *swi2Δ10R* mutant and wild-type cells in any parameter measured in our assay. It could be that Sir3 is still successfully removed from nucleosomes at *HML in vivo* by another nucleosome remodeling complex. Alternatively, Sir3 removal from nucleosomes may not be critical for homologous recombination between the pseudo-*MAT* locus and *HML::cre,* similar to the *in vivo* findings in the Manning and Peterson study. In either case, the inability of Swi2 to interact with Sir3 did not greatly affect the likelihood of silencing loss at *HML::cre* after homologous recombination.

2.5.4 Double-strand-break induction kinetics

Kinetic studies of HO-mediated cleavage of the endogenous *MAT* locus, where it is possible to distinguish the uncut *MAT****a*** and repaired *MAT****α***, report that full cleavage is achieved after approximately 30 minutes of *HO* induction (Hicks *et al.* 2011), yet at no time did I see complete cleavage of the pseudo-*MAT* locus, and the percentage of cleaved pseudo-*MAT* molecules never exceeded 40% throughout the time course. In our study, DNA-blot analysis could not distinguish molecules that had been cleaved and repaired from those that were never cleaved due to the sequence identity between the initial and repaired pseudo-*MAT* products. Thus, it was not clear whether double-strand break induction at our pseudo-*MAT* locus was slower than at the endogenous *MAT* locus, or whether cleavage kinetics were similar to those previously reported. It was also possible that the cleaved pseudo-*MAT* molecules seen at later time points reflect molecules that had been repaired by recombination but without gene conversion, leaving the HO recognition sequence intact for further rounds of cleavage. One would expect that after an adequate time of HO expression, all pseudo-*MAT* molecules would show gene conversion to the un-cleavable SNP-INC sequence found at the donor *HML::cre* locus.

2.5.5 Genetic and phenotypic heterogeneity within colonies

Silencing loss and recombination events were assayed in colonies grown after *HO* induction, representing a temporal difference in the occurrence of these events and their detection. Interestingly, many colonies displayed genotypic and phenotypic heterogeneity regarding the repaired sequence at pseudo-*MAT* and the silencing loss from *HML::cre*.

Approximately half of gene conversion events at pseudo-*MAT* after a 1-hour *HO* induction were partial gene conversion events, in which both the original pseudo-*MAT* and the donor *HML::cre* sequences were detected in a single colony. One possible explanation for this genetic heterogeneity within a single colony could be that recombination in the founder cell led to a mismatch at pseudo-*MAT* that was not resolved prior to replication, causing both alleles to be propagated in the colony. Additionally, the partial gene conversion events may have resulted from differences in the way a founder cell experienced HO-mediated double-strand breaks or subsequent repair from its progeny. Perhaps the HO protein was asymmetrically distributed to either the mother or daughter cell, which could result in one cell experiencing a double-strand break but not the other. In this scenario, the genetic heterogeneity within a colony would result from different events in the first cells that form the colony rather than a single event that leads to two molecular outcomes. It was unlikely that this genetic heterogeneity was due exclusively to the propensity of cells to remain attached after rounds of cell division, because micromanipulating single cells onto solid medium after HO induction to ensure a single founder cell still gave rise to colonies with partial gene conversion events.

The appearance of colonies with silencing loss events that occurred after the

first cell division on the plate was unexpected, as cell division would not be expected to progress before repair of the double-strand break. As with the genetic heterogeneity seen within a colony, micromanipulating single cells onto solid medium after *HO* induction still revealed some colonies that were at least one-quarter green but not completely green [Figure 2.12]. It is unclear whether the propagation of cells that both did and did not lose silencing within a single colony was due to a single recombination event at the one-cell stage that led to different silencing outcomes at *HML::cre* in founder cells and their progeny. It is possible that homologous recombination with pseudo-*MAT* affected chromatin at the *HML::cre* locus in a way that did not manifest silencing loss immediately, resulting in a delay in *cre* transcription by one or two cell divisions. Alternatively, founder cells and their progeny may have experienced different likelihoods of double-strand-break induction by HO, or different repair mechanisms of the double-strand break, whereby one cell and not the other experienced a silencing loss event. Despite these nuances, there was a clear causal link between double-strand break repair templated from *HML::cre* and silencing loss.

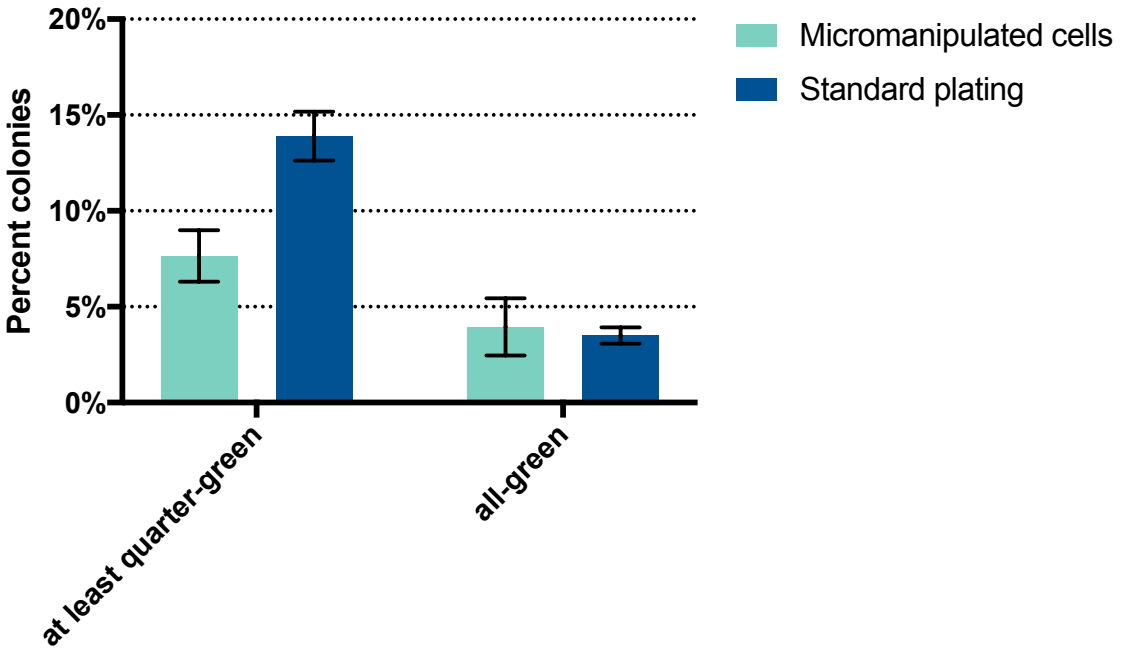

Figure 2.12 Silencing loss patterns in wild-type colonies (JRY10817) after a 1-hour *HO* induction. Colonies that lost silencing were scored as either all-green or at least one-quarter green but not all-green. Cells were either micromanipulated to ensure a single founder cell per colony or plated with a standard glass-bead-spreading technique. Data represented are the means and standard deviations of two biological replicates with 129 micromanipulated colonies total and 699 colonies from standard plating total in the analysis.

2.5.6 Implications beyond *S. cerevisiae*

In this study, homologous recombination targeted to *HML* led to an increased likelihood of transcriptional silencing loss in many, but not all, cells. The silencing loss that did occur at *HML* after homologous recombination was transient and limited, which likely resulted from the efficiency and rapid kinetics with which yeast cells can establish silencing *de novo* when all necessary components are available (Osborne *et al.* 2009). In organisms or genetic backgrounds that cannot rapidly re-establish transcriptional silencing within heterochromatic loci, homologous recombination might alter chromatin structures in a way that has long-lasting effects on the transcriptional output of such loci. Conceivably, other structures of chromatin may also be vulnerable to disruption by homologous recombination. This possibility may become evident with the increase in frequency of Cas9-mediated genome editing studies.

2.5.7 Thoughts on the future of silencing and homologous recombination

This study revealed perturbations to silent chromatin following homologous recombination that had previously escaped detection. Many cells experienced silencing loss following the DNA transactions at *HML* when it served as a donor locus for recombination, yet many others maintained silencing through and after homologous recombination. Understanding what, mechanistically, led to silencing loss after homology-directed repair remains a promising avenue of research to elucidate novel proteins and/or processes with the potential to disrupt silent chromatin.

Many of the experiments in this study involved inducing a double-strand break in liquid culture and measuring silencing-loss events in colonies that were grown on solid medium following double-strand break induction. Quite surprisingly, colonies arose with both genotypic and phenotypic heterogeneity, whereby cells that both did and did not experience silencing loss and/or evidence of homologous recombination were propagated within a single colony. This phenomenon was not solely explained by the possibility that cells failed to separate fully after cell division, as it could be seen even in colonies that arose from a single founder cell. Thus, data interpretation was limited by the inability to tie one repair event to one silencing outcome. Understanding exactly the rate of silencing loss after a single recombination event would bring insight to formulate hypotheses about what could be driving whether or not silencing is lost after recombination.

Future experiments that observe post-recombination silencing loss at the level of individual cells rather than colonies would help to shed light on the actual rate of silencing loss at *HML* following recombination. One potential assay improvement could be a microfluidics-based imaging setup. Single cells captured on a microfluidics chip could experience double-strand break formation at pseudo-*MAT* in the same way that was done in this study, with a switch in medium flowing through the microfluidics chamber to control expression of *pGAL10:HO*. Alternatively, single-molecule mRNA FISH could be performed on cells immediately fixed after double-strand break induction to better observe the landscape of transcription events at the single-cell level.

The ability to retroactively determine in which cells recombination events with *HML* occurred, as was done in this study by extraction of DNA from colonies, would not be possible with a single-cell imaging approach. Thus, a microscopy-based assay would also require modifications to be able to determine which cells successfully templated homologous recombination from *HML.* Tagging various repair proteins with fluorescent epitopes could allow one to determine which cells received a double-strand break at pseudo-*MAT* (Lisby *et al.* 2004), and perhaps in combination with a *dnl4Δ* mutant that is defective in non-homologous end joining could be an accurate indication of which cells underwent homologous recombination at *HML*. With an improved assay to tie one recombination event with one silencing loss

outcome, experiments to understand what influences whether or not a cell loses silencing after recombination could be more informative.

In addition to the hypotheses tested in this study, a handful of interesting explanations for what leads (or doesn't) to silencing loss after recombination remain untested. One appealing hypothesis to explain why a cell does or does not maintain silencing through homologous recombination is that the cell cycle timing of the double-strand break and/or completion of double-strand break repair dictates the silencing outcome. Many proteins are cell-cycle regulated, including the deacetylase Hst3, which is known to contribute to silencing stability through its removal of acetyl marks on histone H3 lysine 56 (Dodson and Rine 2015). It's also possible that homologous recombination at *HML* leads to changes in post-translational histone modifications that disrupt silencing. For example, nucleosomes within *HML* might become hyperacetylated at H3K56 after homologous recombination, requiring Hst3 to restore the chromatin to a state that permits transcriptional silencing. Perhaps the cells that complete recombination when Hst3 is available are those that can escape silencing loss, while those that must wait to remove H3K56 acetylation experience destabilization of silencing and transient transcription at *HML*. In an ideal (and futuristic) experiment, one would be able to observe a silenced cell that undergoes homologous recombination at *HML*, then immediately measure changes to chromatin (nucleosome occupancy, post-translational histone modifications, etc) at *HML*.

Another remaining hypothesis for what determines the outcome to silencing after recombination is that different repair mechanisms influence the likelihood of silencing loss. While mating-type switching exclusively proceeds via the synthesis-dependent strand annealing (SDSA) mechanism of homologous recombination, it could be that different sets of repair proteins disrupt silencing to different degrees. One could observe different recombination events at *HML* executed with different repair mechanisms and different repair proteins, then measure whether silencing loss follows. In another ideal (and futuristic) experiment, one would be able to observe exactly which repair proteins interact with *HML* during recombination and exactly which regions of DNA within *HML* are involved in the recombination event, then detect whether changes in transcriptional silencing follow.

As of now, our understanding of what causes silencing loss after homologous recombination could be viewed as stochastic, as the mechanistic explanation remains elusive. With the rapid innovation of single-cell and single-molecule studies, we may soon approach a detailed understanding of how various aspects of homologous recombination influence the biology of silent chromatin.

Chapter 3

Additional Studies on the Intersection of Homologous Recombination and Silencing

3.1 Introduction

In addition to the experiments described in the previous chapter, I explored the effects of homologous recombination within heterochromatin on silencing using a plasmid-based transformation assay in combination with the CRASH assay. With this approach, I also investigated whether aspects of yeast transformation, or the DNA helicase Mph1, contributed to silencing instability at *HML::cre*. Lastly, I tested whether the presence of the silencing proteins at *HML::cre* impacted its efficiency as a donor template for homologous recombination.

3.2 Materials and Methods

Table 3.1: Yeast strains used in this chapter

Name	Genotype	Source
JRY9627	*matΔ::NatMX, lys2, ura3Δ::pGPD:loxP:yEmRFP;tCYC1:KanMX:loxP:yEGFP:tADH1, can1-100, his3-11, leu2-3,112*	Dodson and Rine 2015
JRy9628	*matΔ::NatMX, lys2, hmlα2Δ::CRE, ura3Δ::pGPD:loxP:yEmRFP;tCYC1:KanMX:loxP:yEGFP:tADH1, can1-100, his3-11, leu2-3,112*	Dodson and Rine 2015
JRY10829	*matΔ::NatMX, lys2, hoΔ::K.l.LEU2, hmlα2Δ::CRE, ura3Δ::pGPD:loxP:yEmRFP;tCYC1:KanMX:loxP:yEGFP:tADH1, can1-100, his3-11, leu2-3,112*	This study
JRY10829	*matΔ::NatMX, lys2, mph1Δ::K.l.LEU2, hmlα2Δ::CRE, ura3Δ::pGPD:loxP:yEmRFP;tCYC1:KanMX:loxP:yEGFP:tADH1, can1-100, his3-11, leu2-3,112*	This study
JRY9633	*matΔ::NatMX, lys2, sir2Δ::HygMX, hmlα2Δ::CRE, ura3Δ::pGPD:loxP:yEmRFP;tCYC1:KanMX:loxP:yEGFP:tADH1, can1-100, his3-11, leu2-3,112*	Dodson and Rine 2015

Table 3.2: Plasmids used in this chapter

Name	Description	Source
pJR3423	*cre-STOP-SNPs URA3 ampR CEN/ARS*	This study
pJR3424	*cre-STOP URA3 ampR CEN/ARS*	This study
pJR3426	*ho-SNPs URA3 ampR CEN/ARS*	This study
pRS313	*HIS3 ampR CEN/ARS*	Sikorski and Hieter 1989

For plasmids pJR3423 and pJR3424, the stop codon in *cre* was a T to G mutation at base-pair 222.
For plasmid pJR3423, the three SNPs within *cre,* referred to collectively in Table 3.2 as SNPs, were as follows: C to T at base-pair 411, T to C at base-pair 459, and G to A at base-pair 765.

For plasmid pJR3426, the first 1,739 base-pairs of the *ho* sequence in W303 were cloned into the XhoI and SacI sites in pRS316. The following mutations were then made: T352 was deleted to create an XbaI site, A to G at base-pair 833 of the original sequence, T to C at base-pair 899 of the original sequence, C to T at base-pair 1265 of the original sequence, and C to A at base-pair 1499 of the original sequence to create a HindIII site.

Transformation of linearized plasmids

Yeast transformations were performed with the lithium acetate/single-strand carrier DNA/PEG method (Gietz 2014). For linearized plasmids, either 3ug or 300ng of restriction digested and gel-purified plasmid was transformed into mid-log phase cells and plated on CSM-Trp-Ura to select for the plasmid.

Colony imaging and silencing loss analysis

Colonies that were imaged for fluorescence were grown for approximately 3 days at 30°C, then imaged on a Typhoon Trio (GE Healthcare) and analyzed manually for sectoring patterns.

Testing effects of transformation reagents and procedures on silencing loss

For the experiments that tested whether the presence of carrier DNA influenced the likelihood of silencing loss after transformation, a transformation with 300 ng of linearized plasmid DNA was executed either with or without 10 ul of 10 mg/ml boiled salmon sperm DNA, and cells were plated on medium selecting for the plasmid.

The experiment to test for heat shock effects on silencing loss was performed by addition of all transformation reagents (sans DNA to be transformed) to cells, which were then plated on non-selective medium. The experiment to test the presence of lithium acetate on silencing loss was performed by adding all other transformation reagents (sans DNA to be transformed), then application of a 42°C heat shock for 40 minutes, which is the temperature and time used in all of the transformation-based experiments. Cells were then plated on CSM-Trp non-selective medium.

Co-transformation experiments

For the co-transformation experiments described in figure 3.7, mid-log phase cells were transformed with 300 ng of intact pRS313 and 300 ng of linearized pJR3423, then plated on CSM-His medium to select for uptake of pRS313. After three days, colonies were replica plated onto CSM-Ura medium, and the fraction of Ura^+ to His^+ colonies was determined. For the co-transformation experiment with intact pJR3423, 300 ng of plasmid was used.

3.3 Results

3.3.1 Design of a gapped-plasmid repair assay to test for silencing loss at *HML::cre* after homologous recombination

To investigate further whether homologous recombination within silent chromatin led to silencing instability, we directed homologous recombination to *HML::cre* via transformation of a linearized plasmid with homology to the *cre* sequence within *HML.* A *CEN-ARS* plasmid was linearized using restriction enzymes, creating a gap in the plasmid's *cre* sequence that could be repaired by homologous recombination with *HML::cre* after transformation (Figure 3.1A). A *URA3* marker allowed me to observe cells that had repaired the linearized plasmid by growing colonies on medium lacking uracil. To ask whether homology-directed repair targeted elsewhere in the genome could disrupt silencing, I transformed a linearized *CEN-ARS* plasmid with homology to the *ho* locus on chromosome IV (Figure 3.1B) and analyzed silencing loss at *HML::cre*. Within the sequence that was removed during the restriction-enzyme-mediated linearization process of both plasmids, I placed three single-nucleotide polymorphisms (SNPs) that allowed us to determine whether Ura^+ colonies had undergone recombination, as homology-directed repair would lead to gene conversion of the plasmids' SNPs. To control for aspects of the transformation process that might result in silencing loss, I performed a mock transformation with no DNA and analyzed silencing loss at *HML::cre* after growth on non-selective medium. Transformation of intact pJR3423 and mock transformation of a strain lacking the *cre* sequence at *HML* yielded no colonies with detectable GFP signal, demonstrating the inability of recombination between *LoxP* sites without Cre protein to activate GFP expression at frequencies that could obscure this analysis (Table 3.3).

Transformation conditions	Colonies imaged	Colonies with GFP signal
mock (no DNA)	13,443	0
pAD39	8,747	0

Table 3.3 In a strain with wild-type *HML* (JRY9627), LoxP sites did not recombine at a detectable frequency without Cre protein after mock transformation or transformation with pJR3424, bearing an early stop codon in the *cre* ORF.

3.3.2 Transformation destabilized silencing at *HML::cre*, and recombination with *HML::cre* further increased silencing loss

Prior to transformation, an average of 2.6% of colonies were all-green, indicative of cells that had already lost silencing at the time of plating (Figure 3.1C). Mock transformation increased the number of all-green colonies to approximately 10% of the population, demonstrating an ability of the transformation process itself to destabilize silencing, a result I further explore later. The presence of intact DNA with homology to *HML::cre* did not result in silencing loss beyond the background levels caused by the transformation process, as transformation with intact pJR3423 led to similar levels of silencing loss as the mock transformation.. In contrast, transformation with linearized pJR3423 led to silencing loss in approximately 36% of Ura^+ colonies. Thus, colonies experienced a greater likelihood of silencing loss when required to repair the linearized plasmid.

One possible explanation for the increase in silencing loss after transformation of linearized pJR3423 was that either the presence of, or the repair of any broken DNA molecule led to destabilization of silent chromatin at *HML::cre*. However, transforming linearized pJR3426, which targeted homology-directed repair to the *ho* locus on a different chromosome, resulted in similar levels of silencing loss as transformation of intact pJR3426. Thus, homology-directed repair within *HML::cre* was required to decrease silencing stability.

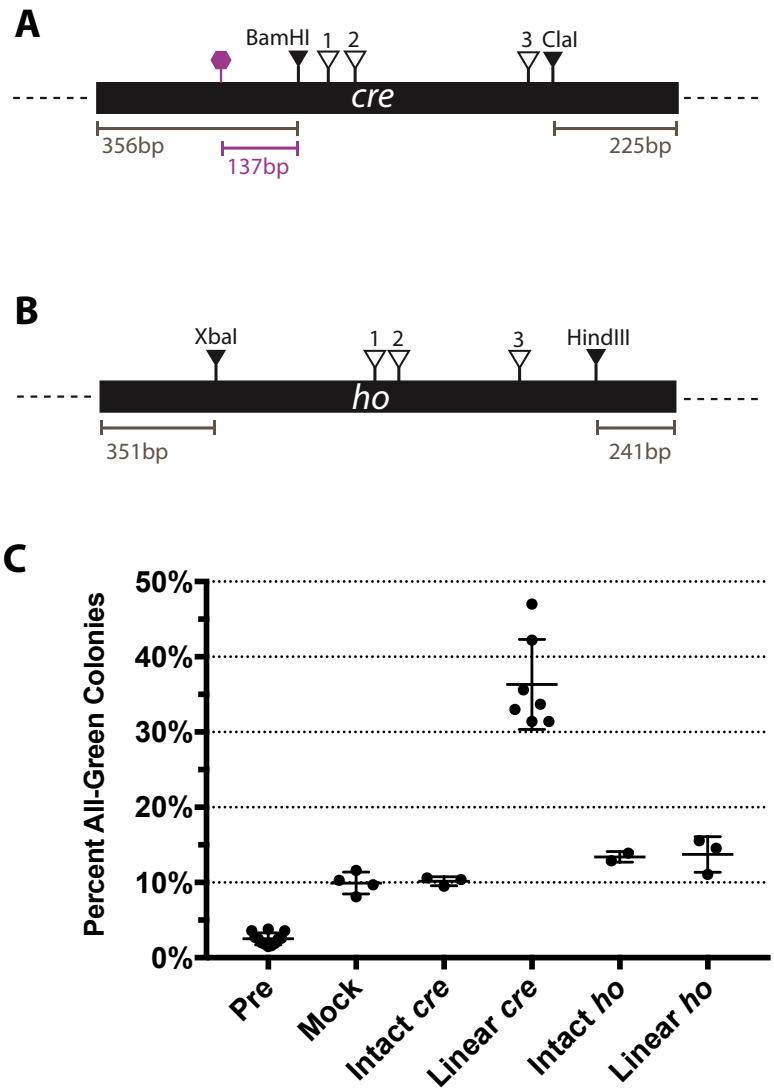

Figure 3.1 (A) Diagram of the *cre* sequence in pJR3423 to direct homology with *HML::cre*. The closed triangles represent the BamHI and ClaI restriction sites used to linearize the plasmid. The purple hexagon represents an early stop codon engineered in place of the Tyr74 residue of the *cre* coding sequence, 137 base-pairs from the BamHI recognition sequence. The open triangles represent SNPs within the *cre* sequence at base-pairs 411 (SNP1), 459 (SNP2), and 765 (SNP3). (B) Diagram of the *ho* sequence in pJR3426 to direct homology at the *ho* locus on chromosome IV. The closed triangles represent the XbaI and HindIII restriction sites used to linearize the

plasmid. The open triangles represent SNPs within the *ho* sequence at base-pairs 833 (SNP1), 899 (SNP2), and 1265 (SNP3). (C) Percent of all-green colonies before transformation (pre), after a mock transformation with no DNA, and after transformation with intact and linearized *cre* and *ho* plasmids. Each dot represents a biological replicate, and a minimum of 308 colonies was analyzed for each replicate. Horizontal lines for each condition represent the means and standard deviation of each replicate. Colonies analyzed for the pre- and mock transformation conditions were grown on non-selective medium, and colonies analyzed after transformation with plasmid DNA were grown on medium lacking uracil.

3.3.3 Gapped-plasmid repair proceeded exclusively through homologous recombination rather than non-homologous end joining

Repair of linearized plasmid DNA can proceed by a mechanism other than homologous recombination, namely non-homologous end joining (NHEJ). To estimate the number of Ura$^+$ colonies that had not undergone recombination at their target locus, I transformed linearized plasmid DNA into a strain lacking any homologous sequence that could be used for a repair template. When linearized pJR3423 was introduced into a strain with wild-type *HML* (JRY9627), the number of colony-forming units (CFUs) on –uracil medium was 7% that of the same linearized pJR3423 transformed into a strain with *HML::cre* (Figure 3.2). Thus, the potential for false-positive Ura$^+$ colonies that did not undergo homologous recombination with *HML::cre* likely did not exceed 7% of the total population. When linearized pJR3426 was transformed into a strain lacking an *ho* sequence to template homology-directed repair (JRY10828), the efficiency of colony growth on –uracil medium was less than 1% relative to transformation with a strain bearing the *ho* locus. These data suggest that the vast majority of colonies that grew on the –uracil selective medium after transformation had indeed undergone homologous recombination between the linearized plasmid and its intended genomic repair template.

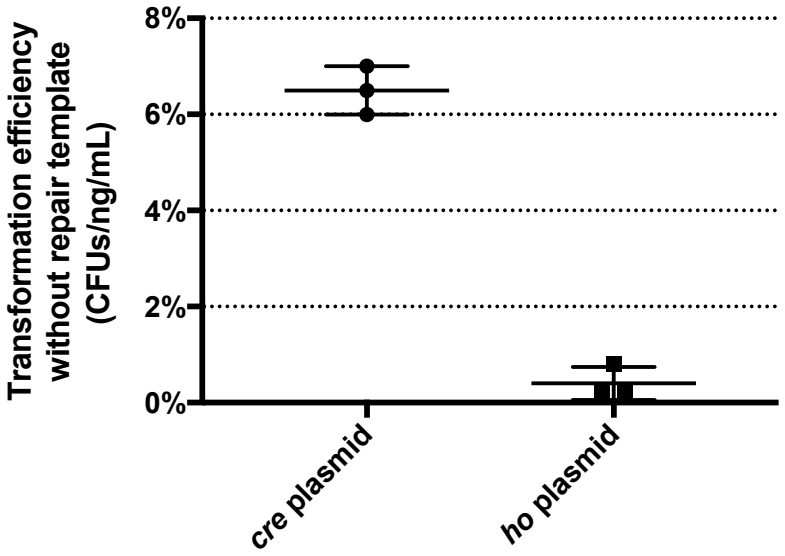

Figure 3.2 Percentage of CFUs on selective medium when linearized plasmid was transformed into a strain lacking a homologous repair template relative to one that allowed homology-directed repair (JRY9627 vs JRY9268 for the *cre* plasmid and JRY10828 vs JRY9628 for the *ho* plasmid). Each dot represents an independent biological replicate. For each replicate, a minimum of 1,379 colonies was analyzed.

Homology-directed repair of the linearized plasmids would result in gene conversion of the SNPs located between the restriction sites used for linearization, as recombination would replace the excised sequence with that of the homologous template. To determine more directly the frequency of homologous recombination between the linearized plasmids and targeted template loci, I sequenced the pJR3423 and pJR3426 plasmids in Ura$^+$ colonies after transformation.

After transformation of linearized pJR3423 into JRY9628, I observed gene conversion of at least one of the four SNPs distinguishing the original plasmid sequence from *HML::cre* in every plasmid sequenced (Figures 3.3A and 3.3B). In almost all instances, all three SNPs between the BamHI and ClaI sites converted to the *HML::cre* sequence, although one repaired plasmid showed conversion of only one of the SNPs. Approximately 20% of Ura$^+$ colonies sequenced had also gene converted the stop codon within the *cre* sequence of pJR3423. Gene conversion of the stop codon was equally likely in colonies that did or did not lose silencing, indicating that the presence of the promoterless wild-type *cre* sequence in the repaired pJR3423 did not affect the likelihood of silencing loss. Interestingly, all of the red colonies that maintained silencing through the transformation process had also successfully templated homologous recombination at *HML::cre*. Thus, recombination between the linearized plasmid and *HML::cre* did not require an obligate loss of silencing.

Homologous recombination targeted to the *ho* locus was also highly efficient, as 100% of plasmids sequenced from Ura+ colonies showed gene conversion of the excised SNPs (Figures 3.3C and 3.3D). Additionally, all plasmids sequenced had gene converted the SNPs used to create the XbaI and HindIII sites that were not present at the endogenous *ho* locus.

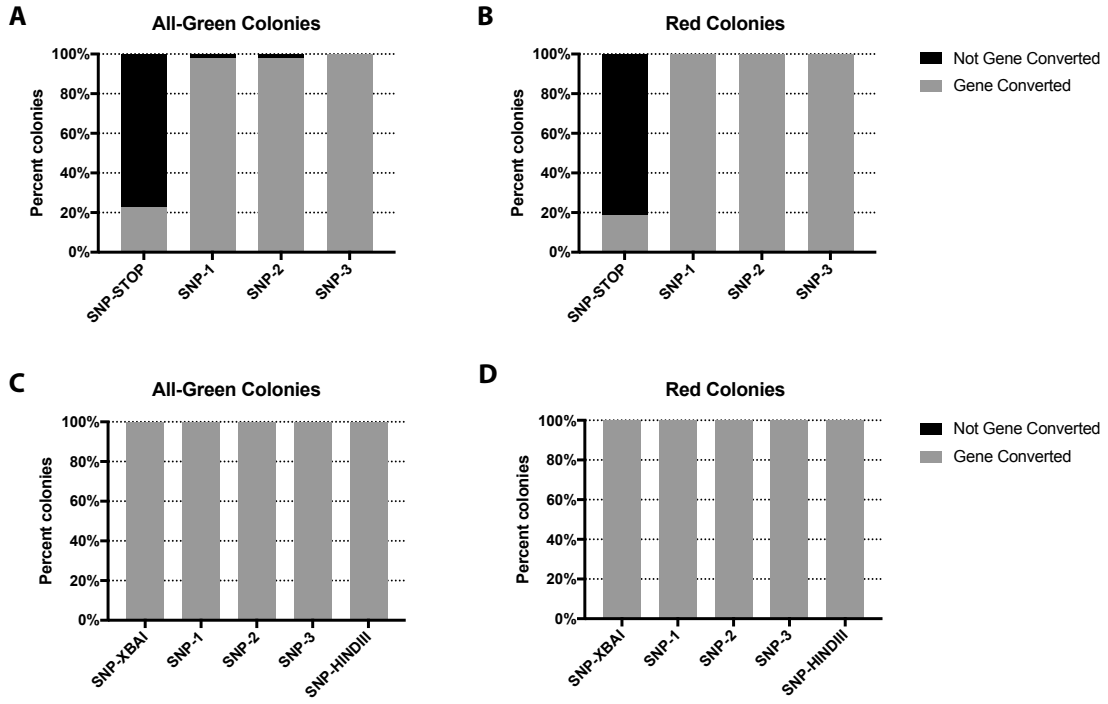

Figure 3.3 Gene conversion frequencies in plasmids from either all-green or red colonies after transformation of pJR3423 (panels A and B) and pJR3426 (panels C and D) into JRY9628. Sequences from 44 (A), 43 (B), 18 (C), and 14 (D) colonies are represented in these data.

3.3.4 Certain aspects of the transformation process could destabilize silencing

The transformation process used to introduce the linearized plasmids involved exposure to at least three reagents/conditions with the potential to explain the silencing instability resulting from transformation: heat shock, lithium acetate, and carrier DNA. To test which, if any, of these led to increased silencing loss at *HML::cre*, I first repeated the mock transformation while omitting either the exposure to heat shock or the addition of lithium acetate. When all transformation reagents were added but cells were not heat shocked, there was no increase in silencing loss levels above the pre-transformation background levels (Figure 3.4). Exposure to heat shock without lithium acetate caused an increase in silencing instability above

background levels, but did not reach the level of silencing loss seen with the full mock transformation. Thus, heat shock was necessary but not sufficient for silencing loss caused by the transformation process, and exposure to lithium acetate did not cause destabilization of silencing at *HML::cre*.

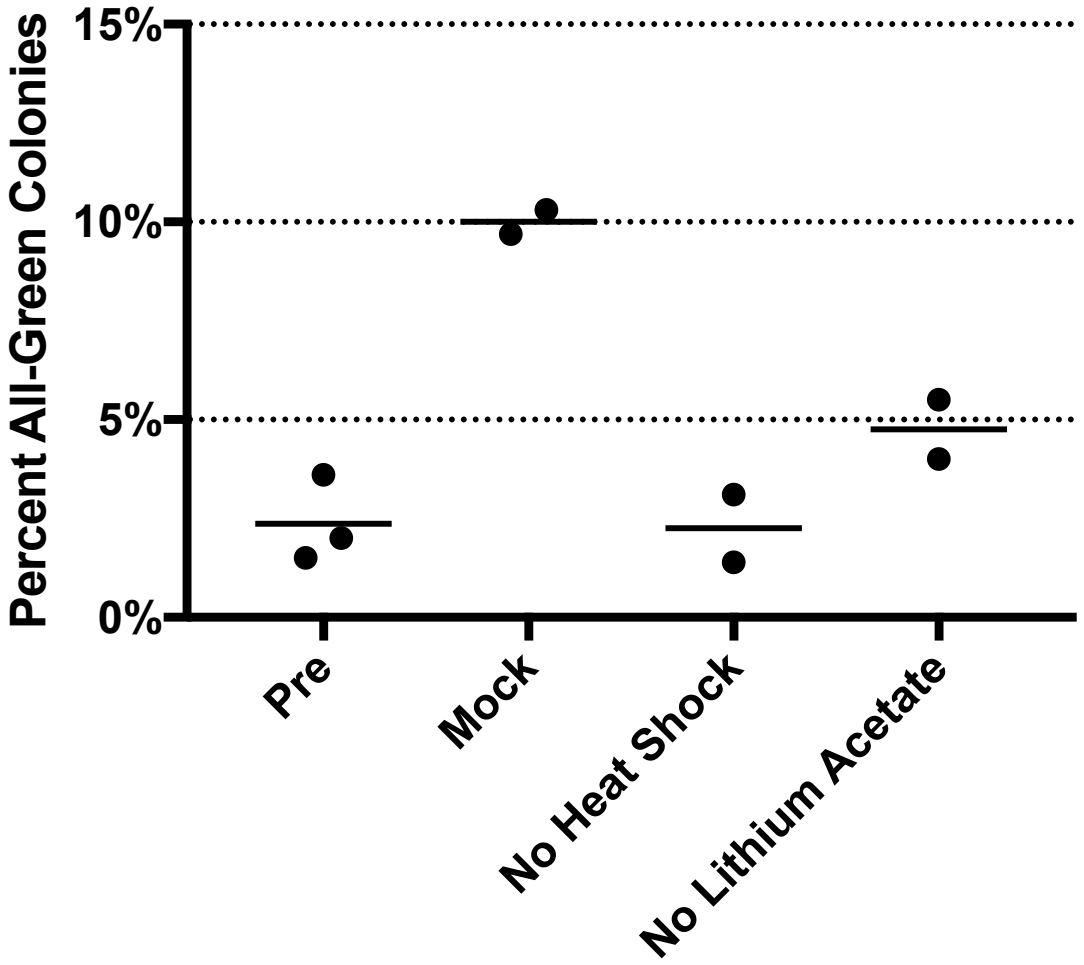

Figure 3.4 Effects of mock transformation, heat shock, and lithium acetate exposure on silencing stability at *HML::cre*. Each dot represents a biological replicate, and horizontal lines represent means of replicates. A minimum of 1,813 colonies was analyzed for each replicate.

I next tested the effects on silencing at *HML::cre* of carrier DNA in the transformation process. I transformed linearized pJR3423 DNA with and without the presence of carrier DNA and saw similar levels of silencing loss in Ura+ colonies (Figure 3.5A). The absence of carrier DNA decreased the efficiency of transformation itself: the percentage of Ura+ CFUs from a transformation without carrier DNA was small relative to transformation with carrier DNA (Figure 3.5B). Aside from reducing

the transformation efficiency, the presence of carrier DNA did not influence the frequency of silencing loss, suggesting that it was not responsible for the increased silencing loss seen in the mock transformation process.

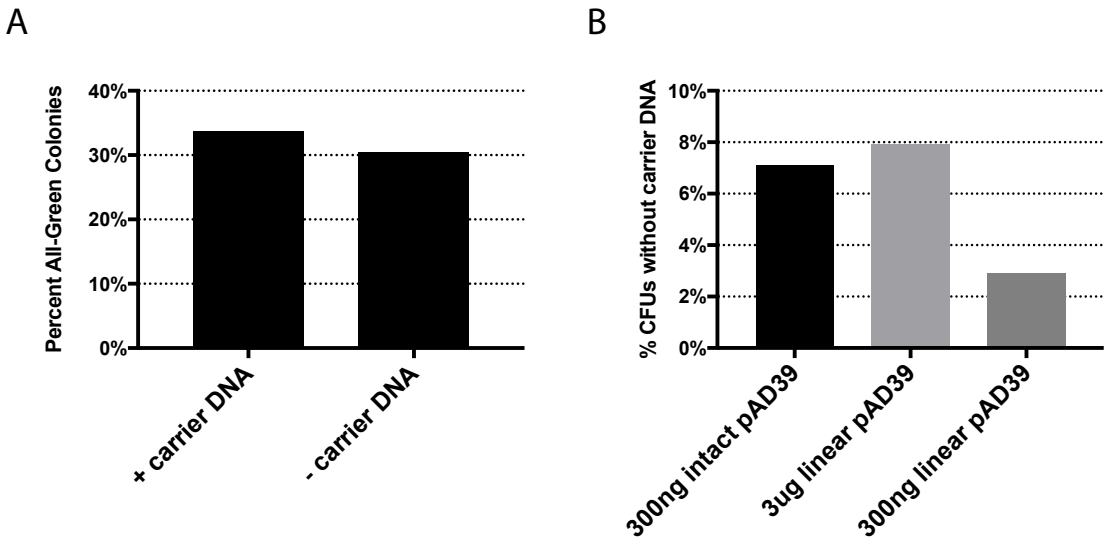

Figure 3.5 Effects of carrier DNA on silencing loss after transformation with linearized pJR3424 (A) and transformation efficiency of intact and linearized pJR3424 (B). 2,156 colonies with carrier DNA and 171 colonies without carrier DNA were analyzed in panel A, and a minimum of 308 colonies was analyzed for each condition in panel B. All conditions represent one biological replicate.

3.3.5 Effects of *mph1Δ* on silencing loss after transformation

Homology-directed repair of linearized pJR3423 decreased silencing stability in many cells, but a majority maintained silencing after engaging in homologous recombination at *HML::cre*. Homologous recombination can proceed via multiple mechanisms (reviewed in Pâques and Haber 1999), including synthesis-dependent strand annealing (SDSA), double-Holliday junction formation with and without reciprocal crossover, and Holliday junction dissolution. Thus, we hypothesized that differences in repair mechanism might explain the difference in likelihood of silencing loss after recombination at *HML::cre*.

Mph1 is a DNA helicase that promotes repair via SDSA, likely due to its *in vitro* ability to dismantle D-loops (Prakash *et al.* 2009; Zheng *et al.* 2011). *mph1Δ* strains exhibit no decreased ability to repair gapped plasmids through homologous recombination, but increase the frequency of crossover events and Holliday junction dissolution at the expense of SDSA events (Mitchel *et al.* 2013). To ask whether the absence of Mph1 would shift the ratio of red-to-green colonies after homologous recombination, I transformed linearized pJR3423 into an *mph1Δ* mutant (JRY10829). Silencing at *HML::cre* was unaffected in the *mph1*Δ strain, as the pre-transformation

and mock transformation background levels of silencing loss were similar to wild type (Figure 3.6). Transformation with both intact and linearized pJR3423 led to a higher percentage of all-green Ura$^+$ colonies in *mph1Δ* relative to wild type (Figure 3.6 vs Figure 3.1C). Thus, while silencing loss after homologous recombination at *HML::cre* appeared higher in the absence of Mph1, the increased silencing loss after transformation with intact pJR3423 suggests that the silencing instability may not be an effect specific to homology-directed repair.

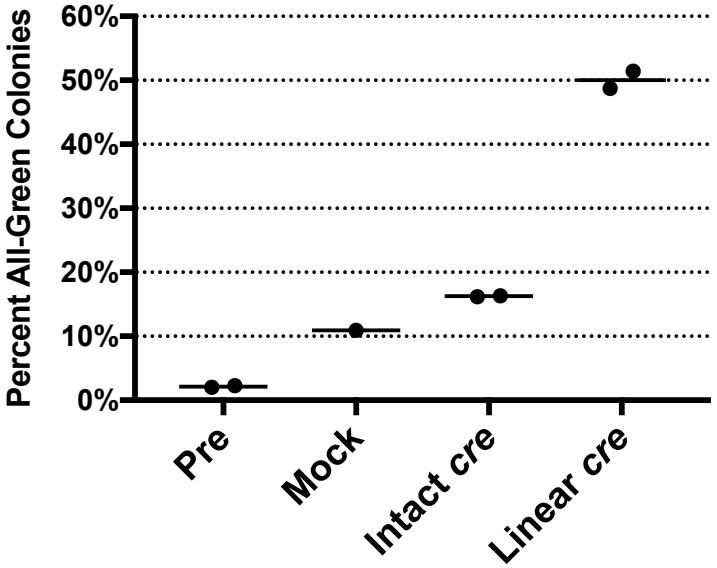

Figure 3.6 Percent of all-green colonies in an *mph1Δ* mutant (JRY10829) before transformation (pre), after mock transformation, and after transformation with intact and linearized pJR3423. Each dot represents a biological replicate, and a minimum of 865 colonies was analyzed for each replicate. Horizontal lines for each condition represent the means of replicates. Colonies analyzed for the pre- and mock transformation conditions were grown on non-selective medium, and colonies analyzed after transformation with plasmid DNA were grown on medium lacking uracil.

3.3.6 Presence of the silencing machinery did not influence efficiency of *HML::cre* as a donor for homologous recombination

Although silent chromatin inhibits access of many DNA-binding proteins to their silenced target sequences, this assay efficiently selected for recombination events with *HML::cre*. Previous studies found an increased efficiency of homologous recombination when a donor locus was actively transcribed relative the same locus without transcription (Saxe *et al.* 2000; Schildkraut *et al.* 2006). Therefore, it is possible that the increase in all-green colonies after repair of linearized pJR3423 reflected a selection for cells with un-silenced *HML::cre* loci that could conceivably be preferred for templating homologous recombination.

To test whether presence of the silencing machinery affected homology-directed repair of linearized pJR3423, we measured repair efficiency in a *sir2Δ* background that lacks transcriptional silencing at *HML::cre*. To control for differences in transformation efficiency, we performed a co-transformation experiment with an intact His+ plasmid alongside either intact or linearized pJR3423 and selected first for growth on medium lacking histidine. We then asked whether colonies that had taken up the *HIS3* plasmid were also Ura^+. When linearized pJR3423 was co-transformed with a *HIS3* plasmid, approximately 1.8% of resulting His^+ colonies were also Ura^+ in *SIR2*, while 3.3% of His^+ colonies were Ura^+ in *sir2Δ* (Figure 3.7). For co-transformation with intact pJR3423, approximately 20.6% of His+ *SIR2* colonies were also Ura^+, and 23.5% of His^+ *sir2Δ* colonies were Ura^+. The slight differences in repair efficiency of linear pJR3423 in the *sir2Δ* strain were not significantly different when analyzed with an unpaired t-test. Thus, the chromatin status of *HML::cre* did not influence the efficiency of homology-directed repair of pJR3423.

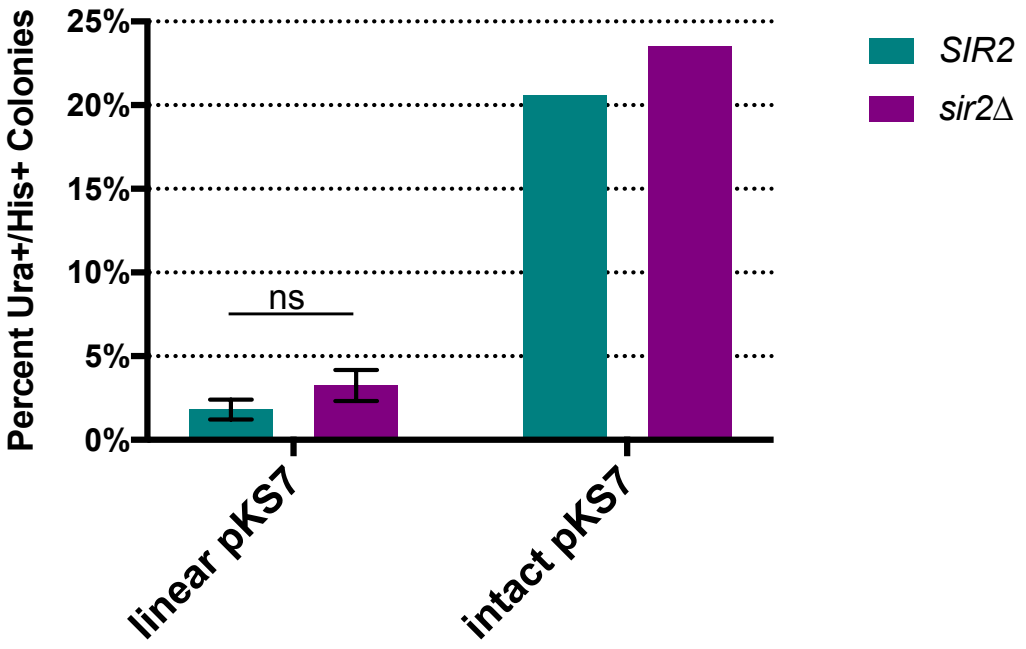

Figure 3.7 Co-transformation efficiencies in *SIR2* (JRY9628) and *sir2Δ* (JRY9633) backgrounds. The percentage of cells selected for their His+ phenotype that were also Ura+ is shown for both linearized pJR3423 and intact pJR3423. For the linear pJR3423 experiment, the means and standard deviations of three independent biological replicates are shown. An unpaired t-test was used to determine that the means were not statistically significantly different. One biological replicate is represented for the intact pJR3423 experiment. A minimum of 1,713 His+ colonies and 1,653 His+ colonies total were analyzed for the linearized and intact pJR3423 experiments, respectively.

3.4 Discussion

3.4.1 Transformation of a linearized plasmid efficiently induced recombination with targeted genomic loci

In this study, I targeted homologous recombination to *HML::cre* by transforming a linearized plasmid containing the *cre* sequence. As a control experiment, I targeted homologous recombination to a different locus in the genome, *ho*. Plating transformed cells on medium lacking uracil allowed selection for colonies arising only from cells with an intact plasmid. I initially estimated a false-positive frequency for Ura+ colonies at around 7% for the *cre* plasmid and 1% for the *ho* plasmid. However, sequencing plasmids recovered from Ura+ colonies revealed that every colony contained a plasmid that was repaired through homologous recombination of its targeted locus. Thus, this transformation assay was highly efficient in selecting for recombination events.

3.4.2 Recombination with *HML::cre* often, but not always, led to silencing loss

Upon imaging the Ura+ colonies to determine whether silencing had been lost at *HML::cre* after it participated in homologous recombination, I found that approximately 33% of colonies were all green and thus had lost silencing before dividing. This represented about a 3-fold increase in silencing loss relative to transformation with an intact plasmid, which resulted in approximately 10% all-green colonies. Interestingly, many of the colonies were still red, indicating persistence of the silent state at *HML::cre* through homology-directed repair. Sequencing plasmids from red colonies further supported our observation that homologous recombination need not always lead to silencing loss, as all of the plasmids from red colonies showed evidence of gene conversion that would result from homology-directed repair.

Recombination targeted to the *ho* locus did not lead to an increase in silencing loss at *HML::cre* beyond that seen after transformation with an intact *ho*-bearing plasmid. Hence, the increase in silencing loss at *HML::cre* after plasmid repair was specific to events that directly involved *HML::cre* as the donor locus.

3.4.3 Aspects of the transformation process could destabilize silencing

In addition to increased silencing instability after *HML::cre* templated homologous recombination, transformation of intact *CEN-ARS* plasmids led to silencing loss in about 10% of colonies. I then performed a "mock" transformation, whereby I exposed cells to the transformation process without adding plasmid DNA. Mock transformation led to the same levels of silencing loss seen with transformation of the intact *CEN-ARS* plasmids, suggesting that the transformation process itself was capable of destabilizing silencing.

I tested three different aspects of the transformation process to determine which, if any, were responsible for the increased silencing loss. The presence of carrier DNA did not change the likelihood of silencing loss after transformation, nor did exposure to lithium acetate without heat shock. Cells that were heat shocked but did not receive lithium acetate experience a slightly greater likelihood of silencing loss, albeit not to the extent seen when all aspects of the transformation are experienced. Thus, the exposure of transformed cells to heat shock was necessary but not sufficient for the increase in silencing loss seen in the mock transformation.

The increase in silencing instability after heat shock may be related to MAPK-dependent phosphorylation of Sir3 (Stone and Pillus 1996). Sir3 hyperphosphorylation increased the strength of telomeric silencing, but has not been studied in the context of silencing at *HML* and *HMR*. It is possible that heat shock-mediated modification of Sir3 leads to structural changes that are not amendable to full silencing at *HML*. The exact cause of silencing instability after heat shock remains unknown.

3.4.4 *mph1Δ* mutants were more sensitive to silencing loss after transformation

The DNA helicase Mph1 promotes homologous recombination via SDSA, the mechanism utilized during mating-type switching. To ask whether mechanism choice during homologous recombination influences the likelihood of silencing loss, I repeated our transformation-based recombination assay in an *mph1Δ* mutant background. Approximately 50% of cells gave rise to all-green colonies after transformation of the linearized *cre* plasmid, which was slightly higher than the approximately 38% of all-green colonies in a wild-type background. However, *mph1Δ* mutant cells experienced slightly higher levels of silencing loss after transformation with the intact *cre* plasmid. It is unclear whether the increased likelihood of silencing loss after transformation of any plasmid DNA explains the increase seen after homology-directed repair of the *cre* plasmid at *HML::cre*, or whether there is a mechanistic difference underlying the higher levels of silencing loss after *HML::cre* participated in homologous recombination. The fold-differences in silencing loss after transformation with linearized versus intact *cre* plasmid were very similar between wild type and *mph1Δ*, suggesting that perhaps the presence of Mph1 did not influence the likelihood of silencing loss at *HML::cre* after templating homologous recombination.

3.4.5 Sir-based silencing did not affect homology-mediated repair efficiency of a linearized plasmid from *HML::cre*

In some assays for homologous recombination, transcription of a donor locus increases its likelihood to template repair. In this study, *HML::cre* was able to template homology-directed repair of a linearized plasmid as efficiently when silenced as unsilenced. Although Sir-based silencing imparts a barrier to many DNA-binding proteins, the machinery required to access *HML::cre* for homologous recombination was not hindered by the presence of Sir proteins. This observation eliminated the hypothesis that the increase in all-green colonies seen after transformation with the linearized *cre* plasmid could be explained by a subset of unsilenced cells that served as more efficient recombination templates. Therefore, recombination induced silencing loss, and silencing loss did not influence recombination.

References

Abraham J., Nasmyth K. A., Strathern J. N., Klar A. J., Hicks J. B., 1984 Regulation of mating-type information in yeast. Negative control requiring sequences both 5' and 3' to the regulated region. J. Mol. Biol. 176: 307–331.

Agmon N., Liefshitz B., Zimmer C., Fabre E., Kupiec M., 2013 Effect of nuclear architecture on the efficiency of double-strand break repair. Nat. Cell Biol. 15: 694–9.

Armache K.-J., Garlick J. D., Canzio D., Narlikar G. J., Kingston R. E., 2011 Structural Basis of Silencing: Sir3 BAH Domain in Complex with a Nucleosome at 3.0 A Resolution. Science (80-.). 334: 977–982.

Bi X., Broach J. R., 1997 DNA in transcriptionally silent chromatin assumes a distinct topology that is sensitive to cell cycle progression. Mol. Cell. Biol. 17: 7077–7087.

Boscheron C., Maillet L., Marcand S., Tsai-Pflugfelder M., Gasser S. M., *et al.*, 1996 Cooperation at a distance between silencers and proto-silencers at the yeast *HML* locus. EMBO J. 15: 2184–2195.

Brand A. H., Breeden L., Abraham J., Sternglanz R., Nasmyth K., 1985 Characterization of a "silencer" in yeast: A DNA sequence with properties opposite to those of a transcriptional enhancer. Cell 41: 41–48.

Brand A. H., Micklem G., Nasmyth K., 1987 A yeast silencer contains sequences that can promote autonomous plasmid replication and transcriptional activation. Cell 51: 709–719.

Braunstein M., Rose A. B., Holmes S. J., Allis C. D., Broach J. R., 1993 Transcriptional silencing in yeast is associated with reduced histone acetylation. Genes Dev. 7: 592–604.

Buchman a R., Kimmerly W. J., Rine J., Kornberg R. D., 1988 Two DNA-binding factors recognize specific sequences at silencers, upstream activating sequences, autonomously replicating sequences, and telomeres in *Saccharomyces cerevisiae*. Mol. Cell. Biol. 8: 210–225.

Chai B., Huang J., Cairns B. R., Laurent B. C., 2005 Distinct roles for the RSC and Swi / Snf ATP-dependent chromatin remodelers in DNA double-strand break repair. Genes Dev. 19: 1656–1661.

Chen L., Widom J., 2005 Mechanism of transcriptional silencing in yeast. Cell 120: 37–48.

Cheng T. H., Li Y.-C., Gartenberg M. R., 1998 Persistence of an alternate chromatin structure at silenced loci *in vitro*. Proc. Natl. Acad. Sci. U. S. A. 96: 343–8.

Cheng T., Gartenberg M., 2000 Yeast heterochromatin is a dynamic structure that requires silencers continuously. Genes Dev.: 452–463.

Chiolo I., Minoda A., Colmenares S. U., Polyzos A., Costes S. V, *et al.*, 2011 Double-strand breaks in heterochromatin move outside of a dynamic HP1a domain to complete recombinational repair. Cell 144: 732–44.

Connolly B., White C. I., Haber J. E., 1988 Physical monitoring of mating type switching in *Saccharomyces cerevisiae*. Mol. Cell. Biol. 8: 2342–2349.

Delgoshaie N., Tang X., Kanshin E. D., Williams E. C., Rudner A. D., *et al.*, 2014 Regulation of the histone deacetylase Hst3 by cyclin-dependent kinases and the ubiquitin ligase SCFCdc4. J. Biol. Chem. 289: 13186–13196.

Dion V., Gasser S. M., 2013 Chromatin movement in the maintenance of genome stability. Cell 152: 1355–64.

Dodson A. E., Rine J., 2015 Heritable capture of heterochromatin dynamics in *Saccharomyces cerevisiae*. eLife 4: 1–22.

Feldman J. B., Hicks J. B., Broach J. R., 1984 Identification of sites required for repression of a silent mating type locus in yeast. J. Mol. Biol. 178: 815–834.

Fishman-Lobell J., Rudin N., Haber J. E., 1992 Two alternative pathways of double-strand break repair that are kinetically separable and independently modulated. Mol. Cell. Biol. 12: 1292–1303.

Gartenberg M. R., Smith J. S., 2016 The nuts and bolts of transcriptionally silent chromatin in *Saccharomyces cerevisiae*. Genetics 203: 1563–1599.

Gibson D. G., Young L., Chuang R.-Y., Venter J. C., Hutchison C. a, *et al.*, 2009 Enzymatic assembly of DNA molecules up to several hundred kilobases. Nat. Methods 6: 343–5.

Gietz R. D., 2014 Yeast transformation by the LiAc/SS carrier DNA/PEG method. Methods Mol. Biol. 1205: 1–12.

Gottschling D. E., Aparicio O. M., Billington B. L., Zakian V. A., 1990 Position effect at *S. cerevisiae* telomeres: Reversible repression of Pol II transcription. Cell 63: 751–762.

Gottschling D. E., 1992 Telomere-proximal DNA in *Saccharomyces cerevisiae* is refractory to methyltransferase activity in vivo. Proc. Natl. Acad. Sci. U. S. A. 89: 4062–5.

Gueldener U., Heinisch J., Koehler G. J., Voss D., Hegemann J. H., 2002 A second set of loxP marker cassettes for Cre-mediated multiple gene knockouts in budding yeast. Nucleic Acids Res. 30: e23.

Haber J. E., Rogers D. T., McCusker J. H., 1980 Homothallic conversions of yeast mating-type genes occur by intrachromosomal recombination. Cell 22: 277–289.

Haber J. E., 2012 Mating-type genes and MAT switching in *Saccharomyces cerevisiae*. Genetics 191: 33–64.

Herskowitz I., Jensen R. E., 1991 Putting the HO gene to work: Practical uses for mating-type switching. Methods Enzymol. 194: 132–146.

Hicks W. M., Yamaguchi M., Haber J. E., 2011 Real-time analysis of double-strand DNA break repair by homologous recombination. Proc. Natl. Acad. Sci. U. S. A. 108: 3108–15.

Holmes S. G., Broach J. R., 1996 Silencers are required for inheritance of the repressed state in yeast. Genes Dev. 10: 1021–1032.

Imai S., Armstrong C. M., Kaeberlein M., Guarente L., 2000 Transcriptional silencing and longevity protein Sir2 is an NAD-dependent histone deacetylase. Nature 403: 795–800.

Ira G., Malkova A., Liberi G., Foiani M., Haber J. E., 2003 Srs2 and Sgs1–Top3 Suppress Crossovers during Double-Strand Break Repair in Yeast. Cell 115: 401–411.

Ira G., Satory D., Haber J. E., 2006 Conservative inheritance of newly synthesized DNA in double-strand break-induced gene conversion. Mol. Cell. Biol. 26: 9424–9.
Jinek M., Chylinski K., Fonfara I., Hauer M., Doudna J. A., *et al.*, 2012 A Programmable Dual-RNA–Guided DNA Endonuclease in Adaptive Bacterial Immunity. 337: 816–822.
Kimmerly W., Buchman A., Kornberg R., Rine J., 1988 Roles of two DNA-binding factors in replication, segregation and transcriptional repression mediated by a yeast silencer. EMBO J. 7: 2241–53.
Klar A. J., Strathern J. N., 1984 Resolution of recombination intermediates generated during yeast mating type switching. Nature 310: 744–748.
Kostriken R., Strathern J. N., Klar A. J. S., Hicks J. B., Heffron F., 1983 A site-specific endonuclease essential for mating-type switching in *Saccharomyces cerevisiae*. Cell 35: 167–174.
Kramer K. M., Brock J. A., Bloom K., Moore J. K., Haber J. E., 1994 Two different types of double-strand breaks in *Saccharomyces cerevisiae* are repaired by similar RAD52-independent, nonhomologous recombination events. Mol. Cell. Biol. 14: 1293–1301.
Landry J., Sutton A., Tafrov S. T., Heller R. C., Stebbins J., *et al.*, 2000 The silencing protein SIR2 and its homologs are NAD-dependent protein deacetylases. Proc. Natl. Acad. Sci. U. S. A. 97: 5807–11.
Lee C.-S., Wang R. W., Chang H.-H., Capurso D., Segal M. R., *et al.*, 2015 Chromosome position determines the success of double-strand break repair. Proc. Natl. Acad. Sci.: 201523660.
Lee M. E., DeLoache W. C., Cervantes B., Dueber J. E., 2015 A Highly Characterized Yeast Toolkit for Modular, Multipart Assembly. ACS Synth. Biol. 4: 975–986.
Li Y., Jin M., O'Laughlin R., Bittihn P., Tsimring L. S., *et al.*, 2017 Multigenerational silencing dynamics control cell aging. Proc. Natl. Acad. Sci. 114: 11253–11258.
Lisby M., Barlow J. H., Burgess R. C., Rothstein R., 2004 Choreography of the DNA damage response: Spatiotemporal relationships among checkpoint and repair proteins. Cell 118: 699–713.
Loo S., Rine J., 1994 Silencers and domains of generalized repression. Science 264: 1768–71.
Lydeard J. R., Lipkin-Moore Z., Sheu Y. J., Stillman B., Burgers P. M., *et al.*, 2010 Break-induced replication requires all essential DNA replication factors except those specific for pre-RC assembly. Genes Dev. 24: 1133–1144.
Lyndaker A. M., Goldfarb T., Alani E., 2008 Mutants defective in Rad1-Rad10-Slx4 exhibit a unique pattern of viability during mating-type switching in *Saccharomyces cerevisiae*. Genetics 179: 1807–1821.
Mahoney D. J., Marquardt R., Shei G. J., Rose a B., Broach J. R., 1991 Mutations in the *HML* E silencer of *Saccharomyces cerevisiae* yield metastable inheritance of transcriptional repression. Genes Dev. 5: 605–615.
Manning B. J., Peterson C. L., 2014 Direct interactions promote eviction of the Sir3 heterochromatin protein by the SWI/SNF chromatin remodeling enzyme. Proc. Natl. Acad. Sci. U. S. A.: 1–6.

Miné-Hattab J., Rothstein R., 2012 Increased chromosome mobility facilitates homology search during recombination. Nat. Cell Biol. 14: 510–7.
Mitchel K., Lehner K., Jinks-Robertson S., 2013 Heteroduplex DNA position defines the roles of the Sgs1, Srs2, and Mph1 helicases in promoting distinct recombination outcomes. PLoS Genet. 9: e1003340.
Moore J. K., Haber J. E., 1996 Cell cycle and genetic requirements of two pathways of nonhomologous end-joining repair of double-strand breaks in *Saccharomyces cerevisiae*. Mol Cell Biol 16: 2164–2173.
Morrison A. J., Highland J., Krogan N. J., Arbel-Eden A., Greenblatt J. F., *et al.*, 2004 INO80 and γ-H2AX interaction links ATP-dependent chromatin remodeling to DNA damage repair. Cell 119: 767–775.
Neumann F. R., Dion V., Gehlen L. R., Tsai-Pflugfelder M., Schmid R., *et al.*, 2012 Targeted INO80 enhances subnuclear chromatin movement and ectopic homologous recombination. Genes Dev. 26: 369–383.
Nickoloff J. A., Singer J. D., Heffron F., 1990 In vivo analysis of the *Saccharomyces cerevisiae* HO nuclease recognition site by site-directed mutagenesis. Mol. Cell. Biol. 10: 1174–9.
Onishi M., Liou G. G., Buchberger J. R., Walz T., Moazed D., 2007 Role of the Conserved Sir3-BAH Domain in Nucleosome Binding and Silent Chromatin Assembly. Mol. Cell 28: 1015–1028.
Osborne E. A., Dudoit S., Rine J., 2009 The establishment of gene silencing at single-cell resolution. Nat. Genet. 41: 800–6.
Pâques F., Haber J. E., 1997 Two pathways for removal of nonhomologous DNA ends during double-strand break repair in *Saccharomyces cerevisiae*. Mol. Cell. Biol. 17: 6765–71.
Pâques F., Haber J. E., 1999 Multiple pathways of recombination induced by double-strand breaks in *Saccharomyces cerevisiae*. Microbiol. Mol. Biol. Rev. 63: 349–404.
Pillus L., Rine J., 1989 Epigenetic inheritance of transcriptional states in *S. cerevisiae*. Cell 59: 637–647.
Prakash R., Satory D., Dray E., Papusha A., Scheller J., *et al.*, 2009 Yeast Mphl helicase dissociates Rad51-made D-loops: Implications for crossover control in mitotic recombination. Genes Dev. 23: 67–79.
Ravindra A., Weiss K., Simpson R. T., 1999 High-resolution structural analysis of chromatin at specific loci: *Saccharomyces cerevisiae* silent mating type locus *HMRa*. Mol. Cell. Biol. 19: 7994–7950.
Rine J., Herskowitz I., 1987 Four genes responsible for a position effect on expression from *HML* and *HMR* in *Saccharomyces cerevisiae*. Genetics 22: 9–22.
Saxe D., Datta A., Jinks-robertson S., 2000 Stimulation of Mitotic Recombination Events by High Levels of RNA Polymerase II Transcription in Yeast. Mol. Cell. Biol. 20.
Schildkraut E., Miller C. A., Nickoloff J. A., 2006 Transcription of a donor enhances its use during double-strand break-induced gene conversion in human cells. Mol. Cell. Biol. 26: 3098–105.

Sekinger E. A., Gross D. S., 2001 Silenced chromatin is permissive to activator binding and PIC recruitment. Cell 105: 403–414.
Shroff, R., Arbel-Eden, A., Pilch, D., Ira, G., Bonner, W. M., Petrini, J. H., Haber, J. E., Lichten, M, 2004 Distribution and Dynamics of Chromatin Modification Induced by a Defined DNA Double-Strand Break. Curr. Biol. 14: 1703-1711.
Singh J., Klar A. J., 1992 Active genes in budding yeast display enhanced *in vivo* accessibility to foreign DNA methylases: a novel in vivo probe for chromatin structure of yeast. Genes Dev. 6: 186–196.
Sinha M., Watanabe S., Johnson A., Moazed D., Peterson C. L., 2009 Recombinational repair within heterochromatin requires ATP-dependent chromatin remodeling. Cell 138: 1109–21.
Smith J. S., Brachmann C. B., Celic I., Kenna M. A., Muhammad S., *et al.*, 2000 A phylogenetically conserved NAD+-dependent protein deacetylase activity in the Sir2 protein family. Proc. Natl. Acad. Sci. U. S. A. 97: 6658–63.
Southern E., 2006 Southern blotting. Nat. Protoc. 1: 518–525.
Steakley D. L., Rine J., 2015 On the Mechanism of Gene Silencing in *Saccharomyces cerevisiae*. G3; Genes|Genomes|Genetics 5: 1751–1763.
Stone E. M., Pillus L., 1996 Activation of an MAP kinase cascade leads to Sir3p hyperphosphorylation and strengthens transcriptional silencing. J. Cell Biol. 135: 571–583.
Strathern J. N., Herskowitz I., 1979 Asymmetry and directionality in production of new cell types during clonal growth: the switching pattern of homothallic yeast. Cell 17: 371–381.
Strathern J. N., Klar A. J., Hicks J. B., Abraham J. a, Ivy J. M., *et al.*, 1982 Homothallic switching of yeast mating type cassettes is initiated by a double-stranded cut in the *MAT* locus. Cell 31: 183–92.
Sugawara N., Wang X., Haber J. E., Bai Y., Symington L. S., *et al.*, 2003 *In Vivo* Roles of Rad52, Rad54, and Rad55 Proteins in Rad51-Mediated Recombination. Mol. Cell 12: 209–219.
Suka N., Suka Y., Carmen A. A., Wu J., Grunstein M., 2001 Highly specific antibodies determine histone acetylation site usage in yeast heterochromatin and euchromatin. Mol. Cell 8: 473–479.
Sun H., Treco D., Szostak J. W., 1991 Extensive 3′-overhanging, single-stranded DNA associated with the meiosis-specific double-strand breaks at the *ARG4* recombination initiation site. Cell 64: 1155–1161.
Thurtle D. M., Rine J., 2014 The molecular topography of silenced chromatin in *Saccharomyces cerevisiae*. Genes Dev. 28: 245–258.
Tsukuda T., Fleming A. B., Nickoloff J. A., Osley M. A., 2005 Chromatin remodelling at a DNA double-strand break site in *Saccharomyces cerevisiae*. Nature 438: 379–83.
Tsukuda T., Lo Y.-C., Krishna S., Sterk R., Osley M. A., *et al.*, 2009 INO80-dependent chromatin remodeling regulates early and late stages of mitotic homologous recombination. DNA Repair (Amst). 8: 360–9.
Wang X., Haber J. E., 2004 Role of *Saccharomyces* single-stranded DNA-binding protein RPA in the strand invasion step of double-strand break repair. PLoS Biol.

2: 104–112.
Weiss K., Simpson R. T., 1998 High-resolution structural analysis of chromatin at specific loci: *Saccharomyces cerevisiae* silent mating type locus *HMLalpha*. Mol. Cell. Biol. 18: 5392–5403.
White C. I., Haber J. E., 1990 Intermediates of recombination during mating type switching in *Saccharomyces cerevisiae*. EMBO J. 9: 663–673.
Wilson T. E., Grawunder U., Lieber M. R., 1997 Yeast DNA ligase IV mediates non-homologous DNA end joining. Nature 388: 495–8.
Wolner B., Komen S. Van, Sung P., Peterson C. L., 2003 Recruitment of the recombinational repair machinery to a DNA double-strand break in yeast. Mol. Cell 12: 221–232.
Wu X., Haber J. E., 1996 A 700 bp cis-acting region controls mating-type dependent recombination along the entire left arm of yeast chromosome III. Cell 87: 277–285.
Xu E. Y., Zawadzki K. A., Broach J. R., 2006 Single-cell observations reveal intermediate transcriptional silencing states. Mol. Cell 23: 219–29.
Zheng X. F., Prakash R., Saro D., Longerich S., Niu H., *et al.*, 2011 Processing of DNA structures via DNA unwinding and branch migration by the *S. cerevisiae* Mph1 protein. DNA Repair (Amst). 10: 1034–1043.